Accepted Manuscript

CCR2 mediates dendritic cell recruitment to the human colon but is not responsible for differences observed in dendritic cell subsets, phenotype and function between the proximal and distal colon

David Bernardo, Lydia Durant, Elizabeth R. Mann, Elizabeth Bassity, Enrique Montalvillo, Ripple Man, Rakesh Vora, Durga Reddi, Fahri Bayiroglu, Luis Fernández-Salazar, Nick R. English, Simon T.C. Peake, Jon Landy, Gui H. Lee, George Malietzis, Yi Harn Siaw, Aravinth U. Murugananthan, Phil Hendy, Eva Sánchez-Recio, Robin K.S. Phillips, Jose A. Garrote, Paul Scott, Julian Parkhill, Malte Paulsen, Ailsa L. Hart, Hafid O. Al-Hassi, Eduardo Arranz, Alan W. Walker, Simon R. Carding, Stella C. Knight

PII: S2352-345X(15)00151-4
DOI: 10.1016/j.jcmgh.2015.08.006
Reference: JCMGH 72

To appear in: *Cellular and Molecular Gastroenterology and Hepatology*
Accepted Date: 21 August 2015

Please cite this article as: Bernardo D, Durant L, Mann ER, Bassity E, Montalvillo E, Man R, Vora R, Reddi D, Bayiroglu F, Fernández-Salazar L, English NR, Peake STC, Landy J, Lee GH, Malietzis G, Siaw YH, Murugananthan AU, Hendy P, Sánchez-Recio E, Phillips RKS, Garrote JA, Scott P, Parkhill J, Paulsen M, Hart AL, Al-Hassi HO, Arranz E, Walker AW, Carding SR, Knight SC, CCR2 mediates dendritic cell recruitment to the human colon but is not responsible for differences observed in dendritic cell subsets, phenotype and function between the proximal and distal colon, *Cellular and Molecular Gastroenterology and Hepatology* (2015), doi: 10.1016/j.jcmgh.2015.08.006.

Title: CCR2 mediates dendritic cell recruitment to the human colon but is not responsible for differences observed in dendritic cell subsets, phenotype and function between the proximal and distal colon.

Authors: David Bernardo[1*], Lydia Durant[1], Elizabeth R Mann[1,2], Elizabeth Bassity[3], Enrique Montalvillo[4], Ripple Man[5], Rakesh Vora[1,5], Durga Reddi[1], Fahri Bayiroglu[6,7], Luis Fernández-Salazar[8], Nick R English[1], Simon TC Peake[1,5], Jon Landy[1,5], Gui H Lee[1,5], George Malietzis[1,5], Yi Harn Siaw[1,5], Aravinth U Murugananthan[1,5], Phil Hendy[1,5], Eva Sánchez-Recio[1], Robin KS Phillips[7], Jose A Garrote[3,9], Paul Scott[10], Julian Parkhill[10], Malte Paulsen[11], Ailsa L Hart[7], Hafid O Al-Hassi[1], Eduardo Arranz[2], Alan W Walker[10,12], Simon R Carding[3,13], Stella C Knight[1]

Affiliations:

1 Antigen Presentation Research Group, Imperial College London, Northwick Park and St. Mark's Campus, Harrow, HA1 3UJ, UK.
2 Centre for Immunobiology, Institute of Infection, Immunity and Inflammation, University of Glasgow, Glasgow, G12 8TA, UK
3 Gut Health and Food Safety Programme, Institute of Food Research, Norwich, UK
4 Mucosal Immunology Group, Instituto de Biología y Genética Molecular (IBGM), Universidad de Valladolid-CSIC, Valladolid, Spain.
5 St. Mark's Hospital, North West London Hospitals NHS Trust, Harrow, UK.
6 Department of Physiology, Faculty of Medicine, Yildirim Beyazit University, Ankara, Turkey.
7 Faculty of Farmacy, Agri İbrahim Cecen University, Agri, Turkey.
8 Gastroenterology Service, Hospital Clínico Universitario de Valladolid, Valladolid, Spain.
9 Genetics and Molecular Biology Department, Clinical Laboratory Service, Hospital Universitario Rio Hortega, Valladolid, Spain.
10 Pathogen Genomics Group, Wellcome Trust Sanger Institute, Wellcome Trust Genome Campus, Hinxton, Cambridgeshire, CB10 1SA, UK
11 National Heart and Lung Institute, Imperial College London, FACS Laboratory Suite, St. Mary's Campus
12 Microbiology Group, Rowett Institute of Nutrition and Health, University of Aberdeen, Greenburn Road, Aberdeen, AB21 9SB, UK
13 Norwich Medical School, University of East Anglia, Norwich, UK

*Author´s Current Address: Gastroenterology Unit. Hospital Universitario de La Princesa and Instituto de Investigación Sanitaria Princesa (IIS-IP), Centro de Investigación Biomédica en Red de Enfermedades Hepáticas y Digestivas (CIBEREHD). Madrid, 28006, Spain.

Grant support:
The authors gratefully acknowledge the support of the Biotechnology and Biological Sciences Research Council (BBSRC). This research was funded by the BBSRC Institute Strategic Programme for Gut Health and Food Safety BB/J004529/1. Funding for PS, JP, AWW and 16S rRNA gene sequencing was provided by the Wellcome Trust (grant number WT 098051). AWW and the Rowett Institute of Nutrition and Health, University of Aberdeen, receive core funding support from the Scottish Government Rural and Environmental Science and Analysis Service (RESAS). HOA was funded by the Association for International Cancer Research (AICR), Scotland, grant number 120234. The authors also thank the Junta de Castilla y León (Spain, SAN196/VA16/07 and SAN196/VA17/07), and the Wellcome Trust Sanger Institute's core sequencing teams for generating sequence data.

Abbreviations:

CFSE: Carboxyfluorescein succinimidyl ester
DC: Dendritic cells
GI: Gastrointestinal
LPMC: Lamina propia mononuclear cells
Mφ: Macrophages
mDC: Myeloid dendritic cell
pDC: Plasmacytoid dendritic cell
RALDH-2: Retinaldehyde dehydrogenase type 2
T-reg: Regulatory T-cells.

Corresponding author:
Stella C. Knight, Antigen Presentation Research Group, Imperial College London, Northwick Park and St. Mark's Campus, Watford Road, Harrow, HA1 3UJ, UK.
Phone +44 (0) 20 8869 2; Fax +44 (0) 20 8869 3532
Email s.knight@imperial.ac.uk

Disclosures
No author has any conflict of interest to disclose

Author contribution
DB designed the experiments and performed them in collaboration with LD, ERM, EM, FB, ESR, DR, MP and HOA who provided essential support in several experiments and help with data analysis/interpretation. EB and SRC performed the animal model experiments while NRE conducted the electron microscopy experiments. PS prepared the microbiota samples for sequencing. AWW performed the microbiota sequence analyses. RV, PH, RM, LFS, STCP, JL, GHL, GM, YHS RV and ALH performed sample recruitment ensuring that all the collected samples had been obtained from healthy controls with no known autoimmune diseases or malignancies, and with both macroscopically and microscopically normal tissue structure. RSKP, SRC, JAG, EA, ALH and SCK oversaw the design and interpretation of all the studies and provided support with data analysis. Manuscript was drafted by DB and all authors reviewed, discussed and approved the manuscript. JP, SRC, JAG, EA and SCK obtained the funds to perform the experiments.

ABSTRACT

Background & aims: Most knowledge about gastrointestinal (GI)-tract dendritic cells (DC) relies on murine studies where $CD103^+$ DC specialize in generating immune tolerance with the functionality of $CD11b^{+/-}$ subsets being unclear. Information about human GI-DC is scarce, especially regarding regional specifications. Here, we characterized human DC properties throughout the human colon.

Methods: Paired proximal (right/ascending) and distal (left/descending) human colonic biopsies from 95 healthy subjects were taken; DC were assessed by flow cytometry and microbiota composition assessed by 16S rRNA gene sequencing.

Results: Colonic DC identified were myeloid (mDC, $CD11c^+CD123^-$) and further divided based on CD103 and SIRPα (human analog of murine CD11b) expression. $CD103^-SIRP\alpha^+$ DC were the major population and with $CD103^+SIRP\alpha^+$ DC were $CD1c^+ILT3^+CCR2^+$ (although CCR2 was not expressed on all $CD103^+SIRP\alpha^+$ DC). $CD103^+SIRP\alpha^-$ DC constituted a minor subset that were $CD141^+ILT3^-CCR2^-$. Proximal colon samples had higher total DC counts and fewer $CD103^+SIRP\alpha^+$ cells. Proximal colon DC were more mature than distal DC with higher stimulatory capacity for $CD4^+CD45RA^+$ T-cells. However, DC and DC-invoked T-cell expression of mucosal homing markers (β7, CCR9) was lower for proximal DC. CCR2 was expressed on circulating $CD1c^+$, but not $CD141^+$ mDC, and mediated DC recruitment by colonic culture supernatants in transwell assays. Proximal colon DC produced higher levels of cytokines. Mucosal microbiota profiling showed a lower microbiota load in the proximal colon, but with no differences in microbiota composition between compartments.

Conclusions: Proximal colonic DC subsets differ from those in distal colon being more mature. Targeted immunotherapy using DC in T-cell mediated GI-tract inflammation may therefore need to reflect this immune compartmentalization.

Keywords: human gastrointestinal tract; dendritic cells; proximal colon; distal colon; microbiota, CCR2

Synopsis

Intestinal dendritic cells (DC) maintain a balance between tolerance of nutrients/commensals and immunity against pathogens. Here, we report lower numbers of $CD103^{+}SIRP\alpha^{+}$ DC, with a more mature phenotype and higher immune activity, in the proximal than in the distal healthy human colon.

INTRODUCTION

Dendritic cells (DC), unique in their ability to generate primary T-cell mediated immune responses and potent promoters of secondary activity, dictate whether immune responses are immunogenic or tolerogenic and determine their tissue specificity[1]. In the gastrointestinal (GI) tract, DC maintain a balance between tolerance to nutrients and/or commensal microorganisms (the microbiota) and immunity against pathogens[2-4].

Human myeloid DC (mDC; $CD11c^+$) can be divided into $CD1c^+$ (analogous to mouse $CD11b^+$ specialized for "classical presentation") and $CD141^+$ (analogous to mouse $CD8\alpha^+$ specialized for "cross-presentation")[5]. Most current knowledge about GI-tract DC comes from mice, and typically from the small intestine, where $CD103^+$ DC specialize in generating regulatory T-cell (T-reg) responses critical for prevention of spontaneous inflammation. Some of these properties appear to be maintained in the human GIT-tract[6-8]. Further characterization of murine $CD103^+$ DC revealed that the subset co-expressing $CD11b^+$ is unique to the GI-tract, with the $CD103^+SIRP\alpha^+$ DC subset representing their human counterpart[9]. $CD103^+$ DC as a whole are regulatory, but it is unclear whether or not specific subsets carry out distinct functions since $CD103^+CD11b^+$ DC can control immune tolerance [via retinaldehyde dehydrogenase type 2 (RALDH-2) and retinoic acid production][9-13], but can also induce Th17 responses[14]; this latter property suggests some bystander effect and/or redundancy between subsets. $CD103^-$ DC can also generate retinoic acid and migrate to lymph nodes[15]. Although murine studies further our understanding of GI-tract DC immunology they may not always be relevant to humans[16, 17] as, for example, RALDH-2 activity is not restricted to DC in the human colon but is also expressed in macrophages[18].

Discrepancies between human and murine DC may reflect environmental and tissue differences as most murine studies focus on the small bowel while human studies are usually of the lower GI-tract. There is therefore a need to study human intestinal DC in the context of different anatomical locations as murine DC subsets and function vary throughout

the GI-tract[10, 19, 20]. In agreement with this notion, we have recently showed that human large (colon) and small bowel (terminal ileum) DC have different properties with a lower proportion of DC producing pro-inflammatory cytokines in the human colon compared with the (paired) ileum, coupled with a higher capacity of colonic DC to generate T-reg cells[21]. Moreover, colonic and ileal DC have differential abilities to imprint homing properties on the T-cells they stimulate, suggesting DC compartmentalization through the human GI-tract[21]. These regional differences in human GI-tract DC are in agreement with other observations[9], which together suggest the presence of regional immune specialization in the GI-tract (as reviewed recently by Mowat & Agace[22]).

To further explore the possibility that DC change through the GI-tract we focused on the human colon, which is structured into different areas. After the terminal ileum (small bowel) the colon starts at the cecum, followed by the right or ascending colon, transverse colon, descending colon, sigmoid colon and finally the rectum. The right (ascending or proximal side) and left (descending or distal side) part of the human colon have different physiology, embryological origins, gene expression and epigenetic profiles, microbiota load and microbiota metabolic activities[23-26]. Moreover, proximal and distal colorectal cancers are recognized as different entities with proximal colorectal cancer having a lower prevalence but a worse prognosis[27]. Therefore, DC properties may not only be different between the small and the large bowel[21], but also between different areas of the colon. Our hypothesis is that DC subsets, their phenotype and function change through the human GI-tract and that DC from different colonic compartments have different immunological properties.

MATERIAL AND METHODS

Biological samples

Colonic biopsies were obtained at colonoscopy from a total of 95 healthy controls [44.9% males; 57.9±12.9 years (mean ± standard deviation); age interval 28-81]. All samples were obtained after bowel preparation for colonoscopy, which can have an impact on mucosa-associated microbiota composition[28, 29]. Samples were obtained in all cases following informed consent after ethical approval from the Hospital Clínico Universitario de Valladolid (Spain) or the Outer West London Research Ethics Committee (United Kingdom). Patients had been referred for colorectal cancer screening or due to rectal bleeding or changes in bowel transit. In all cases they had macroscopically and histologically normal intestines. Proximal colon refers to the right or ascending colon (closer to the small intestine) while the distal colon refers to the left or descending colon (closer to the rectum). Paired biopsies from both the distal and proximal colon were collected (maximum of 5 biopsies from each area) in ice-chilled complete medium [Dutch modified RPMI 1640 (Sigma-Aldrich, Dorset, UK) containing 100 µg/mL penicillin/streptomycin, 2 mM L-glutamine, 50 µg/mL gentamicine (Sigma-Aldrich) and 10% foetal calf serum (TCS cellworks, Buckingham, UK)] and processed within 1 hour. Gender did not affect the expression of any of the studied parameters. Age, however, gave a positive correlation in the proximal colon with mRNA expression of e-Cadherin (Pearson's r=0.66, p-value=0.035) and microbiota load as determined by quantifying 16S rRNA (Pearson's r: -0.75, p-value=0.011).

Human peripheral blood was collected from healthy volunteers with no known autoimmune or inflammatory diseases, allergies or malignancies following informed consent. Peripheral blood mononuclear cells (PBMC) were obtained by centrifugation over Ficoll-Paque PLUS (Amersham Biosciences, Chalfont St. Giles, UK). Some PBMC were washed twice in PBS containing 1 mM EDTA and 0.02% sodium azide (FACS buffer) and stained with fluorochrome-conjugated antibodies while others were used to enrich naïve T-cells.

Lamina propria DC

Lamina propria DC were characterized by flow cytometry as previously described[21, 30-32]. Briefly, freshly obtained biopsies were incubated with Hanks balanced salt solution (HBSS) (Gibco BRL, Paisley, Scotland, UK) containing 1 mM DTT for 20 minutes and then in 1 mM EDTA solutions to remove the associated mucus/bacteria and epithelial layer, respectively. Lamina propia mononuclear cells (LPMC) were obtained from biopsy tissue following quick collagenase digestion with 1 mg/mL of collagenase D (Roche Diagnostics Ltd, Lewes, UK). LPMC were collected by centrifugation, washed twice in FACS buffer and stained with fluorochrome-conjugated antibodies. Viable DC were identified by flow cytometry within single live cells as $CD45^+$ $HLA\text{-}DR^+$ lineage $(CD3\ CD14\ CD16\ CD19\ CD34)^-$ based on Forward and Side scatter characteristics (Figure 1a).

In some cases, LPMC were cultured overnight (37 ℃, 5% CO_2, high humidity) and subsequently enriched for DC after density-gradient centrifugation (600 g, 15 min at RT) using NycoPrep™, and were then cultured with T-cells. The cells collected from the interface (typically 25,000-50,000 cells) have been characterized as functional colonic DC[17, 21, 30-34].

Antibody labelling

LPMC and/or PBMC were stained with monoclonal antibodies for DC characterization. Supplementary Table 1 shows the specificity, clone fluorochrome and sources of the antibodies used. Cells were labelled in FACS buffer. Labelling was performed on ice and in the dark for 20 min. Cells were washed twice in FACS buffer, fixed with 1% paraformaldehyde in 0.85% saline and stored at 4 ^{0}C prior to acquisition on the flow cytometer (within 48 hours). Appropriate isotype-matched control antibodies were purchased from the same suppliers. For intracellular staining, cells were fixed with Leucoperm A following surface staining and permeabilized with Leucoperm B before intracellular staining.

Endocytic activity of DCs was determined by uptake of FITC-dextran (molecular weight 40 kDa) (Sigma, UK) (100 µg/ml, 30 minutes at 37 ℃ or on ice (internal contr ol))[21, 33]. Surface staining for flow cytometry acquisition was subsequently performed as above.

Proliferation assays

$CD4^+$ naïve T-cells were obtained from freshly isolated PBMC, suspended in MiniMACs buffer (PBS containing 0.5% BSA and 2 mM EDTA) and depleted of CD14, CD19, CD8, CD45RO and HLA-DR positive cells with immunomagnetic beads (Miltenyi Biotech, Bisley, UK) following the manufacturer's instructions. $CD4^+$ naïve T-cells were labelled with 10 µM 5-carboxyfluorescein diacetate succinimidyl ester (CFSE, Invitrogen Ltd, UK) and cultured ($4x10^5$/well) for 5 days in U-bottomed 96 well microtitre plates (BD) with 0%, 1%, 2% or 3% enriched allogeneic colonic DC. Cells were recovered and $CFSE^{low}$ proliferating cells identified, quantified and phenotyped by flow cytometry.

Culture supernatants

Freshly obtained intestinal biopsies were immediately cultured in complete medium (1 biopsy per 1 ml of complete medium per well) for 24 hours after which culture media were filtered (0.45 µm) and cell-free supernatants preserved (-80 ^oC) until they were analyzed using a FlowCytomix Multiple Analyte Detection (Ebioscience) on a BD CantoII flow cytometer (BD), following the manufacturer´s instructions, for the concentration of interferon (IFN) γ [detection limit (DL): 0.25 pg/ml]; IFNα [DL: 4.04 pg/ml];interleukin (IL)-1β [DL: 1.80 pg/ml]; IL-2 [DL: 0.35 pg/ml]; IL-4 [DL: 1.22 pg/ml]; IL-5 [DL: 0.76 pg/ml]; IL-6 [DL: 4.10 pg/ml]; IL-7 [DL: 3.18 pg/ml]; IL-9 [DL: 1.17 pg/ml]; IL-10 [DL: 2.88 pg/ml]; IL-12p70 [DL: pg/ml]; IL-13 [DL: 0.43 pg/ml]; IL-17A [DL: 0.89 pg/ml]; IL-22 [DL: 3.98 pg/ml]; IL-23 [DL: 29.14 pg/ml]; IL-27 [DL: 0.79 pg/ml]; leptin [DL: 34.95 pg/ml]; and tumour necrosis factor α (TNF-α) [DL: 3.10 pg/ml]. IgA content was determined via radial immunodifussion kit (Kit IgA RID- ML, Binding Site, UK, DL: 8.5 mg/L) following the manufacturer's instructions. Values below the level of detection were reported as being equal to that.

Quantitative Polymerase Chain Reaction

Freshly obtained intestinal biopsies were immediately embedded in RNAlater (Ambion) and snap-frozen (-80 ^{o}C). Total RNA was isolated from each biopsy using the TRIZOL® reagent according to the protocol provided by the manufacturer. Reverse transcription was carried out by using the SuperScript® First-Strand Synthesis System for Reverse Transcriptase (RT)-PCR Kit (Invitrogen, Life Technologies, USA) using random hexamers. mRNA levels of RALDH2, CCL25, MADCAM1, e-Cadherin and GADPH (housekeeping gene), were measured by real-time PCR by using a LightCycler® instrument (Roche Applied Science, Mannheim, Germany). Microbiota load was determined via 16S rRNA amplification. Reactions were performed using the FastStart SYBR Green MasterMix (Roche) with thermolabile Uracil DNA Glycosylase (UDG) (Roche) to prevent carry-over contamination. Primer sets and PCR conditions are described in Supplementary Table 2. Levels are expressed as the ratio molecule/GADPH in arbitrary units (U).

Migration experiments

One million fresh PBMC were placed in the upper insert of transwell culture plates and their capacity to migrate through 3 µm pores assessed by flow cytometry following collection of the cells in the lower chamber. Colonic biopsies from the proximal and distal colon were cultured as above in 24 well culture plates (3 biopsies per well in 1.5 ml of complete medium) for 18 hours after which samples were filtered (0.45 µm) and the cell-free culture supernatants used immediately in the lower chamber of transwell culture plates (Sigma Aldrich). In some experiments, the colonic supernatants were incubated (20 minutes, room temperature) with anti-CCL2 (1 µg/ml) prior to performing the migration experiments. In other cases, the lower chamber contained fresh complete medium supplemented with different doses of human recombinant CCL2. The addition of fluorescent counting beads (Flow-count Fluorospheres, Beckman Coulter, CA, USA) prior to flow cytometry acquisition allowed

determination of the absolute number of migrated cells into the lower chamber. Results are shown as a ratio compared to the basal or spontaneous migration.

Flow cytometry and data analysis

Cells were acquired on a BD Canto II (BD Biosciences) or a LSR Fortessa flow cytometer (BD Biosciences) and analyzed using WinList 3D 7.1 software (Verity, ME, US). The proportion of cells positive for a given marker was determined by reference to staining with an isotype-matched control antibody.

Electron Microscopy

Electron microscopy characterization of colonic DC was done as previously described[21, 33, 35]. Briefly, between 200,000–1,000,000 LPMC were fixed in 3% glutaraldehyde in 0.1 M Sodium phosphate buffer (SPB) pH 7.4 for up to 2 hours at room temperature and then kept at 4 ^{0}C until they were processed. The cells were washed in the 0.1 M pH 7.4 SPB and embedded as a pellet in low gelling temperature agarose (Sigma). They were washed in 0.1 M pH 7.4 Sodium phosphate buffer and post fixed in 1% osmium tetroxide in 0.1% pH 7.4 SPB for 1 hour. The samples were then washed and left in distilled water overnight to remove the phosphate and were block stained in 2% uranyl acetate for 2-4 hours. The samples were washed with dH_2O and dehydrated using an acetone gradient and gradually infiltrated with araldite resin. Araldite was changed twice over 4-8 hours, samples were embedded in the araldite resin and then cured for 18 hours at 65 ℃. Ultrathin sections (100 nm thick) were cut on a Reichert-Jung Ultracut E microtome and collected on a 200 mesh copper grid. After staining with Reynold's lead citrate, the grid was carbon coated and visualized using a JEOL 1200 EX electron microscope. DC were identified as previously described[33-36]. DC were subsequently classified into mature and immature DC based on their morphology by electron microscopy. Immature DC were small cells with short veils relative to their size, a small area of cytoplasm and heterochromatic nuclei with thick chromatin layer surrounding the nucleus

and chromatic dense clusters within the nucleus. In contrast, mature DC had long veiled projections[21].

Microbiota analysis

Paired biopsies from the proximal and distal colon from a total of 19 healthy controls (9 females, 10 males; mean age 59.7±10.2) with no known autoimmune disease and/or malignancies were collected. Biopsies were immediately embedded in RNAlater (Ambion) and snap-frozen at -80 ^{o}C. DNA was extracted using the FastDNA® SPIN Kit for Soil in conjunction with a Fastprep-24 machine (MP Biomedicals) following the manufacturer's protocols.

The V1-V2 regions of bacterial 16S rRNA genes were PCR amplified using Q5^{TM} Taq polymerase (New England Biolabs) and Golay barcoded primers (purchased from Eurofins MWG Operon) MiSeq-27F (5'- AATGATACGGCGACCACCGAGATCTACACTATGGTAATT CCAGMGTTYGATYMTGGCTCAG-3') and MiSeq-338R (5'-CAAGCAGAAGACGGCATACGAGAT-barcode-AGTCAGTCAGAAGCTGCCTCCCGTAGGAGT-3'). Each sample included in the study was amplified with a 338R primer containing a unique 12-mer Golay barcode sequence. PCR conditions were as follows: 98 ºC for 2 mins followed by 25 cycles of 98 ºC for 30 secs, 50 ºC for 30 secs, 72 ºC for 1 min 30 secs and then a final extension step at 72º C for 5 mins. Four PCR reactions per sample were carried out, which were then pooled into a single amplicon mix for each of the samples. PCR amplicons from each sample were then quantified using a Qubit 2.0 Fluorometer (Life Technologies Ltd, Invitrogen Division) and equimolar concentrations of each sample were added together into a final mastermix for sequencing on an Illumina MiSeq machine (2 x 250 bp read length). Sequence data has been deposited in the European Nucleotide Archive under study number ERP007146. The individual accession numbers for each of the biopsy samples are shown in Supplementary Table 3. The resulting sequence data was processed using the mothur software package, closely following their MiSeq SOP[37]. In brief, paired contigs were created from the forward

and reverse MiSeq reads, and all contigs shorter than 260 bp, longer than 450 bp and those containing any ambiguous bases or homopolymeric stretches of longer than 7 bases were removed. Chimeras were removed using Perseus[38] as implemented in mothur. OTUs were generated from pre-clustered data (diffs=3) at the 97% cut-off level and then assigned a taxonomic classification using the RDP taxonomy provided with mothur. Diversity measures such as Shannon and inverse Simpson indices were calculated in mothur, where every sample was first subsampled down to 450 reads to ensure equal sequencing depth for these comparisons. Good's coverage (an estimate of completeness of species sampling) at this sequencing depth was on average 93.4%. A cluster dendrogram, using the Bray Curtis calculator was generated in mothur, and visualised using the iTOL online resource[39]. Differences in bacterial community structure between proximal and distal colonic biopsies were assessed using the AMOVA, parsimony, Metastats[40] and LEfSe[41] tests as implemented in the mothur software package.

Statistical analyses

Two-tailed paired t-test, two-tailed Pearson´s correlation and two-way paired ANOVA were applied as explained in each section/figure legend. In the case of multiple comparisons, subsequent *ad-hoc* Bonferroni correction was applied. Microbiota data was compared using the AMOVA, parsimony, Metastats[40] and LEfSe[41] tests as implemented in the mothur software package[42]. The level of significance was fixed at $p < 0.05$.

RESULTS

Identification of human colonic DC.

Antigen presenting cells ($CD45^+HLA\text{-}DR^{high}$) were identified within LPMC. DC discrimination from macrophages (Mφ) and B-cells was based on lack of expression of markers of other lineages (Figure 1a) as we and others have previously described[17, 18, 21, 31, 32, 34]. DC also had lower granularity as they lack Mφ vacuolar systems, aiding discrimination between DC and Mφ. Further analysis confirmed that DC gated in this way were $CD14^-$ and $CD64^-$ (Figure 1b). Additionally, in contrast to Mφ, DC up-regulated CCR7 expression following 18 hour culture (Figure 1b)[18]. Culture also induced DC maturation (Figure 1c) and these DC were used in functional experiments for T-cell stimulatory capacity[21, 31, 33] avoiding the need for additional exogenous stimulation.

DC numbers were significantly higher in the proximal colon (Figure 1d) with all DC in both compartments being mDC ($CD11c^+CD123^-$) (Figure 1e). The inability to detect non-mDC in human colonic biopsies was not due to sample processing and/or collagenase digestion as this protocol was able to detect pDC in peripheral blood mononuclear cell samples processed in parallel with colonic biopsies (Figure 1e). This is in agreement with recent observations suggesting that non-mDC in the human GI-tract are scarce or absent[18, 43]. Further analysis of colonic mDC confirmed that most were $CD1c^+$ DC and not $CD141^+$ DC (Figure 1f) with no differences between compartments.

Dendritic cell subsets in the human colon

Comparisons of DC subsets derived from the proximal and distal human colon were made based on CD103 and SIRPα expression[9, 21] (Figure 2a). $SIRP\alpha^+$ DC were equally distributed in each compartment but there was a lower proportion of $CD103^+$ DC in the proximal colon biopsies (Figure 2b), which translated into lower numbers of $CD103^+SIRP\alpha^+$ DC (analogous to murine $CD103^+CD11b^+$ DC)[9] at this site (Figure 2c). Further characterization revealed that $SIRP\alpha^+$ DC (both $CD103^+$ and $CD103^-$) were typically $CD1c^+$ while $CD103^+SIRP\alpha^-$ were

CD141$^+$ DC (Figure 2d)[9, 10]. CX3CR1 was virtually absent in all colonic DC (Figure 2e), but was expressed by macrophages[17], while the GI-tract homing β7 integrin was expressed by the majority of colonic DC with all CD103$^+$ DC being positive. SIRPα, which regulates homeostatic properties of intestinal DC[44], was typically co-expressed with the inhibitory receptor ILT3[45], with no differences between CD103$^-$SIRPα$^+$ and CD103$^+$SIRPα$^+$ DC: CD103$^+$SIRPα$^-$ DC were ILT3$^-$. Conversely, ILT3$^-$ DC displayed higher expression of the costimulatory molecule CD40 (Figure 2e).

Having characterized human colonic DC subsets, we next determined whether or not proximal and distal human colonic DC subsets had differences in activation/maturation and homing marker expression. To this end, we examined expression of CD40 (representative of DC maturation status) and β7 (indicative of DC gut-homing capacity) on different DC subsets. Given the low numbers of DC obtained from human colonic biopsies (Figure 1d), and that SIRPα$^-$ cells were scarce in all locations (Figures 2a-c), these markers were studied in CD103$^+$SIRPα$^+$ and CD103$^-$SIRPα$^+$ DC subsets (analogous to murine CD103$^+$CD11b$^+$ and CD103$^+$CD11b$^-$ subsets, respectively)[9] to ensure measurable effects. Both subsets from the proximal colon revealed lower β7 and higher CD40 expression compared with their distal counterparts (Figure 2f) suggesting that alterations in DC exist between proximal and distal compartments of human colon irrespective of the DC subset.

CCR2 mediates DC recruitment in the colon

We next studied the potential mechanisms that may account for blood DC recruitment by the human colon to see whether there was a differential recruitment capacity elicited by the proximal and distal sides. CCR2 mediates monocyte recruitment in the intestinal mucosa, although its expression may not be restricted to monocytes/macrophages as Scott et al have identified a novel CCR2$^+$ DC subset within murine and human intestinal DC[20]. CCR2 was expressed by most colonic CD103$^-$SIRPα$^+$DC with expression being variable on

$CD103^+SIRP\alpha^+$ and absent on $CD103^+SIRP\alpha^-$ DC (Figure 3a), with no differences between the proximal and distal side of the human colon (Figure 3b).

$CCR2^+$ APC numbers are increased in the coeliac duodenum following *in vivo* gluten challenge[46], suggesting intestinal recruitment of blood precursors. We therefore characterized CCR2 expression on human circulating DC. Blood DC were identified within $HLA\text{-}DR^+$ cells (after exclusion of $CD14^+CD16^+CD19^+$ cells) and divided into subsets based on the expression of CD123 (pDC), CD11c/CD1c ($CD1c^+$ mDC) and CD11c/CD141 ($CD141^+$ mDC)[5] (Figure 3c). Circulating $CD1c^+$ mDC were $SIRP\alpha^+ILT3^+CCR2^+$ in contrast to circulating $CD141^+$ mDC, which were $SIRP\alpha^-ILT3^-CCR2^-$ (Figure 3d). Circulating $CD1c^+$ mDC therefore displayed a phenotype similar to intestinal $SIRP\alpha^+$ DC ($CD1c^+ILT3^+CCR2^+$) while circulating $CD141^+$ mDC had a phenotype similar to intestinal $CD103^+SIRP\alpha^-$ DC ($CD141c^+ILT3^-CCR2^-$) (Figures 2 and 3). These results are in agreement with recent observations relating intestinal $SIRP\alpha^+$ DC to circulating $CD1c^+$ mDC and intestinal $CD103^+SIRP\alpha^-$ DC to circulating $CD141^+$ mDC[9].

The similar phenotype of intestinal $SIRP\alpha^+$ DC and circulating $CD1c^+$ mDC, and expression of CCR2 on both DC subsets suggest that they might be recruited to the colonic mucosa in a CCR2 dependent manner. To explore this possibility we first confirmed that CCR2 on circulating mDC was functional; these cells (together with monocytes) migrated in a dose-dependent manner towards CCL2 in transwell migration assays (Figure 3e). Finally, we studied whether cell-free colonic culture supernatants attracted circulating mDC. While circulating monocytes were not attracted by the colonic culture supernatants, DC had a higher migration (compared with the basal) towards distal (p-value = 0.04) and proximal (p-value = 0.06) cell-free culture supernatants; migration was CCR2 dependent as migration was reduced if the culture supernatants had been previously blocked with anti-CCL2 (Figure 3f). These results confirm that CCR2 expression is functional on circulating mDC and that it

mediates blood DC recruitment by the human colon. However, there was no differential capacity of the proximal and distal sides of the colon to recruit circulating DC.

Proximal colon DC are more mature and have lower homing marker expression

Given that there was not a differential capacity to recruit circulating DC by the proximal or distal human colon (Figure 3), and that DC differences between the proximal and distal compartments occurred in all DC subsets (Figure 2f), we next characterized in more detail the phenotype and function of total mDC in each compartment.

As human proximal and distal colon DC expressed different levels of β7 (Figure 2f), we further studied the expression and potential function of gut-homing molecules β7 and CCR9[17, 31] by DC isolated from the proximal compared with the distal colon. MadCam1 (α4β7 ligand) expression was equally distributed throughout the proximal and distal colon although both e-Cadherin (αEβ7 ligand) and CCL25 (CCR9 ligand) mRNA expression were lower in proximal colon DC (Figure 4a). Fitting with the expression patterns of their corresponding ligands, β7 and CCR9 expression were lower amongst DC from the proximal colon, with the skin- and mucosal-homing CLA and CCR10 molecules being absent (Figure 4b).

We next determined if proximal/distal colonic DC had a different maturational status, as suggested by higher CD40 expression displayed by proximal colon DC (Figure 2f). DC in the proximal colon showed higher expression of CD40, CD80 and CD86 and lower endocytic capacity as assessed by uptake of FITC-dextran dye, suggesting greater maturity (Figure 4c). Lamina propria DC were also studied by electron microscopy to further analyse their maturation status as previously reported[21, 35]. There was a higher proportion of mature DC in the proximal colon as identified by their longer veils/dendrites relative to their size and euchromatic nuclei (Figure 4d) [35].

Proximal colonic DC are more stimulatory with lower gut-homing imprinting capacity

Having described differences in the subsets and phenotype of proximal and distal colonic DC, we next studied whether these differences were reflected functionally. Colonic DC were enriched[21, 31, 33] and co-cultured with pre-sorted CFSE-labelled allogeneic $CD4^+CD45RA^+$ T-cells in a mixed leucocyte reaction (Figure 5a). Compared with blood DC, colonic DC display a low stimulatory capacity for naïve $CD4^+$ T-cells[31], which was dose dependent. However, distal colon DC stimulatory capacity was even lower than that of their proximal counterparts (Figure 5a) correlating with their lower levels of maturation markers (Figure 4c). Proximal DC induced a greater proportion of stimulated T-cells to produce IL-17A, with no alterations in production of other measured cytokines (Figure 5b). In agreement with lower homing marker/ligand expression in the proximal colon (Figures 4a-b), proximal DC had lower GI-tract-homing (β7 and CCR9) and higher non-GI-tract-homing (CLA and CCR4) imprinting capacity for stimulated T-cells (Figure 5c). Thus, DC homing imprinting capacity may be not only tissue but also sub-tissue specific.

Differences in the proximal and distal colonic microenvironments

Finally, we studied potential mechanisms that may account for differences between proximal and distal colon DC. Given that there was no differential capacity elicited by the proximal or distal human colon to recruit circulating DC (Figure 3f), we next studied baseline levels of production of soluble immune mediators following *in vitro* culture of colonic biopsies. The proximal samples produced significantly larger amounts of IL-6, IL-22, IL-23, IL-27, leptin (Figure 6a) and IgA (Figure 6b). The proximal colon also had lower levels of RALDH2 mRNA expression (Figure 6c).

We also studied the colonic microbiota, as its activity is known to change through the length of the human GI-tract[26, 47]. We found that the overall mucosa-associated microbiota load was higher in the distal colon (Figure 6d) although 16S rRNA gene sequencing analysis revealed no differences in mucosa-associated microbiota composition between the proximal and

distal colonic mucosae (Figure 6e). Mean Shannon Diversity Index scores, parsimony and AMOVA tests comparing overall diversity and bacterial community structures between proximal/distal colon showed no significant differences, and there were no OTUs or taxonomic groups associated with particular colonic regions. Inter-individual variation was the greatest driver of microbiota clustering patterns (Figure 6e). These results are consistent with many previous studies describing the predominant mucosa-associated bacterial community as host specific and uniformly distributed along the colon whilst being significantly different from the faecal/luminal community[48, 49].

DISCUSSION.

Here, we report that human DC subsets, phenotype and function differed between the proximal (right or ascending) and distal (left or descending) ends of the colon. Our results revealed that the proximal colon contained higher numbers of DC, which were immunologically more active. Thus, DC of the proximal colon showed a specific reduction of $CD103^+SIRP\alpha^+$ DC and were typically more mature, with higher stimulatory capacity for T-cells. However, balancing this increased stimulatory capacity, they had a lower potential to focus immune activity back to the colon, with lower expression of GI-tract homing markers β7 and CCR9, lower mRNA tissue expression of their ligands and lower imprinting capacity of these markers on T-cells they stimulate. Our results also revealed that intestinal $CD103^{+/-}$ $SIRP\alpha^+$ DC were similar to circulating $CD1c^+$ mDC[9] and may enter the colonic mucosa in a CCR2 dependent manner.

Human colon DC were divided into different subsets based on expression of CD103 and SIRPα, with the latter recently re-defined as human analogs of murine CD11b[9, 21]. Although murine $CD103^-CD11b^+$ DC can express intermediate levels of CX3CR1 (although less than in Mφ), CX3CR1 was absent in all human colon DC (Figure 2e)[17]. CD103 (αE) was co-expressed with β7 on DC (Figure 2e) with their abundance being reduced in the proximal colon, in agreement with lower eCadherin mRNA expression (ligand for $CD103^+\beta7^+$) (Figure 4a) in that compartment. Differential $CD103^+$ DC distribution may account for differences in colonic DC function as murine $CD103^-$ DC have increased IL-17 priming capacity[15] as seen here amongst proximal human colonic DC (Figure 5b). SIRPα was equally expressed on proximal and distal colon DC, rendering the proximal colon with a specific reduction of $CD103^+SIRP\alpha^+$. Further analysis confirmed that colonic $CD103^+SIRP\alpha^+$ and $CD103^-SIRP\alpha^+$ DC are $CD1c^+$ while $CD103^+SIRP\alpha^-$ are mainly $CD141^+$, in agreement with recent observations relating intestinal $SIRP\alpha^+$ (both $CD103^+$ and $CD103^-$) to blood $CD1c^+$ mDC and intestinal $CD103^+SIRP\alpha^-$ to blood $CD141^+$ mDC[9, 10]. Indeed, both circulating $CD1c^+$ mDC

and intestinal SIRPα$^+$ were CD1c$^+$SIRPα$^+$ILT3$^+$CCR2$^+$ while circulating CD141$^+$ mDC and intestinal CD103$^+$SIRPα$^-$ were CD141c$^+$SIRPα$^-$ILT3$^-$CCR2$^-$ (Figures 2 and 3). Moreover, circulating CD1c$^+$ mDC were recruited by human colonic culture supernatants in a CCR2 dependent manner (Figure 3g). Given that DC are thought to acquire CD103 once they have entered the mucosa[10] in a RALDH2-dependent manner[50] it may be possible that circulating CD1c$^+$ mDC enter the mucosa as CD103$^-$SIRPα$^+$ DC via CCR2 and subsequently acquire CD103 at the time that they lose CCR2, thus explaining its variable expression on CD103$^+$SIRPα$^+$ DC (Figure 3a-b). The lower expression of intestinal RALDH2 found in the proximal colon (Figure 6c) may also explain the lower proportion of CD103$^+$ DC in that compartment (Figures 2b-c). The additional mechanisms responsible, however, for circulating CD141$^+$ mDC recruitment by the human colon remain elusive as they do not express CCR2; it is likely that other chemokine receptors may be involved in their recruitment.

Scott et al recently reported that intestinal CCR2$^+$ DC were restricted to a fraction of CD103$^-$ SIRPα$^+$ DC (both human and murine) with its expression being absent on the other intestinal subsets[20]. However, in our hands CCR2 was expressed by all CD103$^-$SIRPα$^+$, with expression being variable on CD103$^+$SIRPα$^+$ and absent on CD103$^+$SIRPα$^-$ DC. Further experiments confirmed these results using different CCR2 antibodies (Supplementary Figure 1) potentially eliminating a technical issue. One of the reasons for this discrepancy might be that Scott et al[20] originally described CCR2$^+$CD103$^-$SIRPα$^+$ DC in murine cells and confirmed their presence in human samples using tissue resections from patients suffering from colorectal cancer. In contrast, in this study we used colonic biopsy samples from healthy intestines. Despite providing limited material, this use of normal tissue mitigates against the abnormal effects of disease and treatment that are inherent when using resected tissue, typically derived from patients suffering from acute GI-cancer, inflammatory bowel diseases and/or related diseases. All samples were obtained from patients referred to clinics due to

change in bowel transit, rectal bleeding and/or screening for GI-diseases although in all cases they had normal tissue structure and were therefore considered as normal healthy colonic samples. Comparisons between healthy biopsies and cancer resections would be required to test whether these differences in tissue source are the reason for different results.

DC acquire a "tolerogenic" profile following exposure to soluble factors derived from intestinal epithelial cells[50] while the pro-inflammatory milieu in inflammatory bowel disease may abrogate their function[32, 51]. The proximal colon produced significantly larger amounts of soluble immune mediators (Figures 6a-b) which may be responsible, at least to some extent, for the higher maturation status of proximal DC. RALDH2 promotes conversion of dietary vitamin A into retinoic acid, which mediates several of the tolerogenic properties of GI-DC including their capacity to generate Tregs and induce GI-tract-homing markers on T-cells they stimulate[9-13]. Given that RALDH2 expression was lower in the proximal colon (Figure 6c), and that retinoic acid mediates acquisition of GI-tract homing markers on immune cells, that may also account for the lower expression of GI-tract-homing markers on DC and their lower imprinting capacity on T-cells they stimulate. Lower GI-tract homing expression/imprinting capacity of proximal DC is also coupled with lower mRNA tissue expression of their ligands in the proximal colon (Figure 4a). Therefore, it may be possible that the proximal and distal ends of the colon may use different levels of homing marker/ligand molecules to ensure compartmentalization of immune responses.

In addition to the differences in the cytokine milieu between the proximal and distal human colon, a differential modulatory effect of the colonic microbiota on intestinal DC may contribute. Indeed, the mucosa-associated microbiota load was lower in the proximal colon (Figure 6d)[47]. Despite the similarity in mucosal microbiota composition between the proximal and distal colon (Figure 6e), in agreement with other observations[48, 49], the metabolic output

of the microbiota changes through the length of the GI-tract as dietary compounds are gradually depleted by the microbiota as they pass through the colon[26]. Therefore, the proximal and distal colonic microbiota produce different levels of short-chain fatty acids[52, 53], and/or other extracellular molecular effectors[54], which may modulate DC properties and/or mucosal production of immune mediators (Figures 6a-c). Indeed, we have shown that, similar to human proximal/distal differences reported here, the frequency of DC was higher in the proximal colon of conventionally raised mice, with no differences between proximal and distal compartments in germ-free animals (Supplementary Figure 2). Therefore, regional DC differences throughout the colon might not only be influenced by the cytokine milieu itself but also directly or indirectly by members of the microbiota.

In summary, our data suggest that human blood CD1c^{+} mDC are recruited by the colonic mucosa in a CCR2 dependent manner and confirm that DC subsets, phenotype and function are different between the proximal and distal human colon, and reveal the proximal colon DC as potentially more immunologically active than their distal counterparts. Studies of the immune system of the GI-tract need therefore to take account of the immune compartmentalization throughout its length. Future studies will address whether GI-tract-DC compartmentalization contributes to diseases such as subtypes of inflammatory bowel diseases and/or colorectal cancer where disease is anatomically restricted to different GI locations. Differences in disease incidence and severity could therefore be related to the varying immune activity of different GI-regions.

REFERENCES

1. Stagg AJ, Kamm MA, Knight SC. Intestinal dendritic cells increase T cell expression of alpha4beta7 integrin. Eur J Immunol 2002;32:1445-54.
2. Stagg AJ, Hart AL, Knight SC, et al. The dendritic cell: its role in intestinal inflammation and relationship with gut bacteria. Gut 2003;52:1522-9.
3. Mowat AM. Anatomical basis of tolerance and immunity to intestinal antigens. Nat Rev Immunol 2003;3:331-41.
4. Chirdo FG, Millington OR, Beacock-Sharp H, et al. Immunomodulatory dendritic cells in intestinal lamina propria. Eur J Immunol 2005;35:1831-40.
5. Collin M, Bigley V, Haniffa M, et al. Human dendritic cell deficiency: the missing ID? Nat Rev Immunol 2011;11:575-83.
6. Bogunovic M, Ginhoux F, Helft J, et al. Origin of the lamina propria dendritic cell network. Immunity 2009;31:513-25.
7. Schulz O, Jaensson E, Persson EK, et al. Intestinal CD103+, but not CX3CR1+, antigen sampling cells migrate in lymph and serve classical dendritic cell functions. J Exp Med 2009;206:3101-14.
8. Varol C, Vallon-Eberhard A, Elinav E, et al. Intestinal lamina propria dendritic cell subsets have different origin and functions. Immunity 2009;31:502-12.
9. Watchmaker PB, Lahl K, Lee M, et al. Comparative transcriptional and functional profiling defines conserved programs of intestinal DC differentiation in humans and mice. Nat Immunol 2014;15:98-108.
10. Bekiaris V, Persson EK, Agace WW. Intestinal dendritic cells in the regulation of mucosal immunity. Immunol Rev 2014;260:86-101.
11. Scott CL, Aumeunier AM, Mowat AM. Intestinal CD103+ dendritic cells: master regulators of tolerance? Trends Immunol 2011;32:412-9.
12. Kinnebrew MA, Buffie CG, Diehl GE, et al. Interleukin 23 production by intestinal CD103(+)CD11b(+) dendritic cells in response to bacterial flagellin enhances mucosal innate immune defense. Immunity 2012;36:276-87.
13. Persson EK, Scott CL, Mowat AM, et al. Dendritic cell subsets in the intestinal lamina propria: ontogeny and function. Eur J Immunol 2013;43:3098-107.
14. Persson EK, Uronen-Hansson H, Semmrich M, et al. IRF4 transcription-factor-dependent CD103(+)CD11b(+) dendritic cells drive mucosal T helper 17 cell differentiation. Immunity 2013;38:958-69.
15. Cerovic V, Houston SA, Scott CL, et al. Intestinal CD103(-) dendritic cells migrate in lymph and prime effector T cells. Mucosal Immunol 2013;6:104-13.
16. Gibbons DL, Spencer J. Mouse and human intestinal immunity: same ballpark, different players; different rules, same score. Mucosal Immunol 2011;4:148-57.
17. Mann ER, Landy JD, Bernardo D, et al. Intestinal dendritic cells: their role in intestinal inflammation, manipulation by the gut microbiota and differences between mice and men. Immunol Lett 2013;150:30-40.
18. Sanders TJ, McCarthy NE, Giles EM, et al. Increased production of retinoic acid by intestinal macrophages contributes to their inflammatory phenotype in patients with Crohn's disease. Gastroenterology 2014;146:1278-88 e1-2.
19. Denning TL, Norris BA, Medina-Contreras O, et al. Functional specializations of intestinal dendritic cell and macrophage subsets that control Th17 and regulatory T cell responses are dependent on the T cell/APC ratio, source of mouse strain, and regional localization. J Immunol 2011;187:733-47.
20. Scott CL, Bain CC, Wright PB, et al. CCR2(+)CD103(-) intestinal dendritic cells develop from DC-committed precursors and induce interleukin-17 production by T cells. Mucosal Immunol 2015;8:327-39.
21. Mann ER, Bernardo D, English NR, et al. Compartment-specific immunity in the human gut: properties and functions of dendritic cells in the colon versus the ileum. Gut 2015.

22. Mowat AM, Agace WW. Regional specialization within the intestinal immune system. Nat Rev Immunol 2014;14:667-85.
23. Kaz AM, Wong CJ, Dzieciatkowski S, et al. Patterns of DNA methylation in the normal colon vary by anatomical location, gender, and age. Epigenetics 2014;9:492-502.
24. Eriksson K, Quiding-Jarbrink M, Osek J, et al. Anatomic segmentation of the intestinal immune response in nonhuman primates: differential distribution of B cells after oral and rectal immunizations to sites defined by their source of vascularization. Infect Immun 1999;67:6210-2.
25. Glebov OK, Rodriguez LM, Nakahara K, et al. Distinguishing right from left colon by the pattern of gene expression. Cancer Epidemiol Biomarkers Prev 2003;12:755-62.
26. Cummings JH, Macfarlane GT. The control and consequences of bacterial fermentation in the human colon. J Appl Bacteriol 1991;70:443-59.
27. Bauer KM, Hummon AB, Buechler S. Right-side and left-side colon cancer follow different pathways to relapse. Mol Carcinog 2012;51:411-21.
28. Harrell L, Wang Y, Antonopoulos D, et al. Standard colonic lavage alters the natural state of mucosal-associated microbiota in the human colon. PLoS One 2012;7:e32545.
29. Mai V, Greenwald B, Morris JG, Jr., et al. Effect of bowel preparation and colonoscopy on post-procedure intestinal microbiota composition. Gut 2006;55:1822-3.
30. Hart AL, Al-Hassi HO, Rigby RJ, et al. Characteristics of intestinal dendritic cells in inflammatory bowel diseases. Gastroenterology 2005;129:50-65.
31. Mann ER, Bernardo D, Al-Hassi HO, et al. Human gut-specific homeostatic dendritic cells are generated from blood precursors by the gut microenvironment. Inflamm Bowel Dis 2012;18:1275-86.
32. Al-Hassi HO, Bernardo D, Murugananthan AU, et al. A mechanistic role for leptin in human dendritic cell migration: differences between ileum and colon in health and Crohn's disease. Mucosal Immunol 2013;6:751-61.
33. Bell SJ, Rigby R, English N, et al. Migration and maturation of human colonic dendritic cells. J Immunol 2001;166:4958-67.
34. Al-Hassi HO, Mann ER, Sanchez B, et al. Altered human gut dendritic cell properties in ulcerative colitis are reversed by Lactobacillus plantarum extracellular encrypted peptide STp. Mol Nutr Food Res 2014;58:1132-43.
35. Maroof A, English NR, Bedford PA, et al. Developing dendritic cells become 'lacy' cells packed with fat and glycogen. Immunology 2005;115:473-83.
36. Patterson S, Gross J, Bedford P, et al. Morphology and phenotype of dendritic cells from peripheral blood and their productive and non-productive infection with human immunodeficiency virus type 1. Immunology 1991;72:361-7.
37. Kozich JJ, Westcott SL, Baxter NT, et al. Development of a dual-index sequencing strategy and curation pipeline for analyzing amplicon sequence data on the MiSeq Illumina sequencing platform. Appl Environ Microbiol 2013;79:5112-20.
38. Quince C, Lanzen A, Davenport RJ, et al. Removing noise from pyrosequenced amplicons. BMC Bioinformatics 2011;12:38.
39. Letunic I, Bork P. Interactive Tree Of Life v2: online annotation and display of phylogenetic trees made easy. Nucleic Acids Res 2011;39:W475-8.
40. White JR, Nagarajan N, Pop M. Statistical methods for detecting differentially abundant features in clinical metagenomic samples. PLoS Comput Biol 2009;5:e1000352.
41. Segata N, Izard J, Waldron L, et al. Metagenomic biomarker discovery and explanation. Genome Biol 2011;12:R60.
42. Schloss PD, Westcott SL, Ryabin T, et al. Introducing mothur: open-source, platform-independent, community-supported software for describing and comparing microbial communities. Appl Environ Microbiol 2009;75:7537-41.

43. Raki M, Beitnes AC, Lundin KE, et al. Plasmacytoid dendritic cells are scarcely represented in the human gut mucosa and are not recruited to the celiac lesion. Mucosal Immunol 2013;6:985-92.
44. Scott CL, Murray TF, Beckham KS, et al. Signal Regulatory Protein alpha (SIRPalpha) regulates the homeostasis of CD103 CD11b DCs in the intestinal lamina propria. Eur J Immunol 2014.
45. Chang CC, Ciubotariu R, Manavalan JS, et al. Tolerization of dendritic cells by T(S) cells: the crucial role of inhibitory receptors ILT3 and ILT4. Nat Immunol 2002;3:237-43.
46. Beitnes AC, Raki M, Brottveit M, et al. Rapid accumulation of CD14+CD11c+ dendritic cells in gut mucosa of celiac disease after in vivo gluten challenge. PLoS One 2012;7:e33556.
47. Hayashi H, Takahashi R, Nishi T, et al. Molecular analysis of jejunal, ileal, caecal and recto-sigmoidal human colonic microbiota using 16S rRNA gene libraries and terminal restriction fragment length polymorphism. J Med Microbiol 2005;54:1093-101.
48. Lepage P, Seksik P, Sutren M, et al. Biodiversity of the mucosa-associated microbiota is stable along the distal digestive tract in healthy individuals and patients with IBD. Inflamm Bowel Dis 2005;11:473-80.
49. Eckburg PB, Bik EM, Bernstein CN, et al. Diversity of the human intestinal microbial flora. Science 2005;308:1635-8.
50. Iliev ID, Spadoni I, Mileti E, et al. Human intestinal epithelial cells promote the differentiation of tolerogenic dendritic cells. Gut 2009;58:1481-9.
51. Bernardo D, Vallejo-Diez S, Mann ER, et al. IL-6 promotes immune responses in human ulcerative colitis and induces a skin-homing phenotype in the dendritic cells and Tcells they stimulate. Eur J Immunol 2012;42:1337-53.
52. Arpaia N, Campbell C, Fan X, et al. Metabolites produced by commensal bacteria promote peripheral regulatory T-cell generation. Nature 2013;504:451-5.
53. Smith PM, Howitt MR, Panikov N, et al. The microbial metabolites, short-chain fatty acids, regulate colonic Treg cell homeostasis. Science 2013;341:569-73.
54. Ruiz L, Hevia A, Bernardo D, et al. Extracellular molecular effectors mediating probiotic attributes. FEMS Microbiol Lett 2014.

FIGURE LEGENDS

Figure 1: Identification of human colonic dendritic cells.

(a) Total antigen presenting cells [$CD45^+HLA\text{-}DR^{high}$] were identified within single viable cells (based on the forward/side scatter properties). DC were further discriminated from Mφ based on lineage marker expression (CD3,CD14,CD16,CD19,CD34). **(b)** In contrast to putative macrophages ($CD45^+HLA\text{-}DR^+lineage^+$), DC ($CD45^+HLA\text{-}DR^+lineage^-$) were $CD64^-CD14^-$ and up-regulated CCR7 expression following overnight culture (blue histogram) as well as **(c)** CD40 and CD86, compared with fresh non-cultured cells (red histogram). Shaded histogram in Figures 1b and 1c denote isotypes **(d)** Percentages of DC within the total number of single lamina propria mononuclear cells (LPMC) were higher in the proximal (Prox) colon compared with the distal (Dist) (n=43). **(e)** Lamina propria DC were mainly $CD11c^+$ myeloid DC (mDC). Lack of non-mDC in the human colon was unlikely to be due to sample processing as distribution of $CD11c^+$ and $CD123^+$ blood DC were not altered following DTT + EDTA + collagenase incubation (gut-protocol) of peripheral blood mononuclear cells. **(f)** Most human colonic DC were $CD1c^+$, in contrast to $CD141^+$DC, with no differences between the proximal and distal colon. Data shown in Figures 1b, 1c, and 1e are representative of two independent experiments. Paired t-tests were applied in Figures (d) and (g) and p-values <0.05 were considered significant (****p<0.0001).

Figure 2: Dendritic cell subsets in the human colon.

(a) Dendritic cells (DC) were identified as in Figure 1a and divided into subsets based on expression of CD103 and SIRPα. Relative proportions of DC in subsets in the proximal (Prox) and distal (Dist) human colon are displayed in **(b)** and **(c)**. **(d)** $CD103^-SIRP\alpha^+$, $CD103^+SIRP\alpha^+$ and $CD103^+SIRP\alpha^-$ DC were characterized for CD1c and CD141; and also for **(e)** CX3CR1, ILT3, CD40 and β7. **(f)** $SIRP\alpha^+CD103^-$ and $SIRP\alpha^+CD103^+$ DC subsets were identified as in Figure 2a and β7 and CD40 expression studied in biopsies from the proximal (blue) and distal (red) human colon compared with the isotype (shaded histogram). Results from panels in (d) and (e) are from at least 5 independent experiments while results

from panel (f) are representative of 3 independent experiments. Paired t-test (figure 2b/c) and paired 1-way ANOVA with Bonferroni's ad-hoc analysis (Figure 2d/e) were applied. P-values <0.05 were considered significant (**p<0.01; ***p<0.001; ****p<0.0001).

Figure 3: CCR2 mediates blood dendritic recruitment by the human colon

(a) $CD103^{-}SIRP\alpha^{+}$, $CD103^{+}SIRP\alpha^{+}$ and $CD103^{+}SIRP\alpha^{-}$ DC were identified as in Figure 2a and assessed for the expression of CCR2. Pooled data regarding CCR2 expression on different subsets and in the proximal and distal colon is shown in **b)**. **(c)** Peripheral blood mononuclear cells (PBMC) were studied by flow cytometry. Following exclusion of CD19, CD14 and CD16, dendritic cells (DC) were identified within $HLA\text{-}DR^{+}$ as plasmacytoid (pDC, $CD123^{+}$) and myeloid (mDC, $CD11c^{+}$). mDC were further divided into $CD1c^{+}$ and $CD141^{+}$. **(d)** Expression of SIRPα, ILT3 and CCR2 was determined on peripheral $CD1c^{+}$ mDC, $CD141^{+}$ mDC and pDC. **(e)** One million PBMC were placed in the upper insert of a transwell chamber and their migration towards different concentrations of CCL2 determined 3 hours later. Total migrated $CD11c^{+}HLA\text{-}DR^{+}$ cells were identified by flow cytometry and further divided into monocytes ($CD14^{+}lineage^{+}$) and DC ($CD14^{-}lineage^{-}$). **(g)** Migration of $CCR2^{+}$ monocytes and DC towards cell-free biopsy culture supernatants from the proximal and distal human colon. DC migration was also determined with and without specific blockage of anti-CCL2 in the culture supernatants. Results from the transwell experiments (figures e-f) are displayed as ratio of migrated cells compared to the basal migration (shown as a dot line). Results from panels in (b) and (d) are from at least 5 independent experiments. Results from panel (e) summarize between 3 and 6 independent experiments per condition while results from panel (f) summarize 7 independent experiments. Paired t-tests were applied and p-values <0.05 were considered significant (*p<0.05; **p<0.01; ***p<0.001; ****p<0.0001).

Figure 4: Proximal colon dendritic cells have lower homing marker expression and are more mature

(a) mRNA expression of the gut-homing ligands MADCAM1, e-Cadherin and CCL25 was determined on non-cultured biopsies by RT-qPCR with the results displayed in arbitrary units (U). **(b)** Dendritic cells (DC) from the proximal (Prox) and distal (Dist) human colon were identified as in Figure 1a and the expression of β7, CLA, CCR9 and CCR10 determined by flow cytometry. **(c)** Expression of co-stimulatory molecules (CD40, CD80, CD86) and FITC-dextran endocytic capacity was also determined by flow cytometry. **(d)** Lamina propria dendritic cells were identified by electron microscopy in distal (Dist) and proximal (Prox) human colon biopsy samples. DC were characterized as immature and mature according to heterocromatic/euromatic nuclei and veil/dendrite extension. The percentage of mature DC is referred to the total number of studied DC in the proximal and distal colon. For the flow cytometry experiments (figures b-c) regions were set according to isotype controls (not shown). Histograms show paired results from several independent experiments. Paired t-tests were applied and p-values <0.05 were considered significant (*p<0.05; **p<0.01; ***p<0.01).

Figure 5: Proximal colon dendritic cells are more stimulatory with lower gut-homing imprinting capacity than distal counterparts.

(a) Four hundred thousand CFSE-labelled allogeneic $CD4^+CD45RA^+$ T-cells were cultured with different numbers of paired proximal (Prox) and distal (Dist) human colonic DC and their stimulatory capacity assessed as the percentage of proliferating T-cells ($CD3^+CFSE^{low}$) by flow cytometry. **(b)** Cytokine and **(c)** homing receptor profile of resting (non-stimulated) and dividing T-cells ($CD3^+CFSE^{low}$) stimulated with 3% Prox/Dist colonic DC. Paired two-way ANOVA (Figure 7a) and paired t-tests (Figure 7b/c) were applied. P-values <0.05 were considered significant (*p<0.05; **p<0.01). Dot-plots are representative of 8 independent experiments displayed in the graphics as the mean + standard error.

Figure 6: Differences in the proximal and distal colonic microenvironments.

(a) Fresh paired biopsies from the distal (Dist) and proximal (Prox) human colon were cultured for 24 hours in complete medium and the cell-free culture supernatants assessed for soluble cytokines/adipokines by Multiplex and **(b)** IgA content by radial immunodifussion. **(c)** RALDH2 mRNA expression was determined on non-cultured biopsies by RT-qPCR and results displayed in arbitrary units (U). **d)** Microbiota load, as measured by 16S rRNA quantity, was determined on non-cultured biopsies from the proximal (Prox) and distal (Dist) human colon by RT-qPCR and results displayed in arbitrary units (U). Paired t-tests were applied and p-values <0.05 were considered significant (*p<0.05). **e)** Cluster dendrogram, generated using the Bray Curtis calculator, displaying mucosal-associated microbiota compositional profiles in the human colonic biopsies. Each pair of samples clusters together in the dendrogram, illustrating the large degree of inter-individual variation rather than a signature proximal versus distal colonic bacterial profile. Bacterial families coloured in brown/yellow/orange represent the Bacteroidetes phylum, blue/grey the Firmicutes phylum, red/purple the Proteobacteria phylum and green the Actinobacteria phylum. Paired t-tests were applied in Figure a-d and p-values <0.05 were considered significant (*p<0.05; **p<0.01; ***p<0.001; ****p<0.0001). Results from figures a-d are displayed as mean + standard error of 12 independent experiments.

FIGURE 1

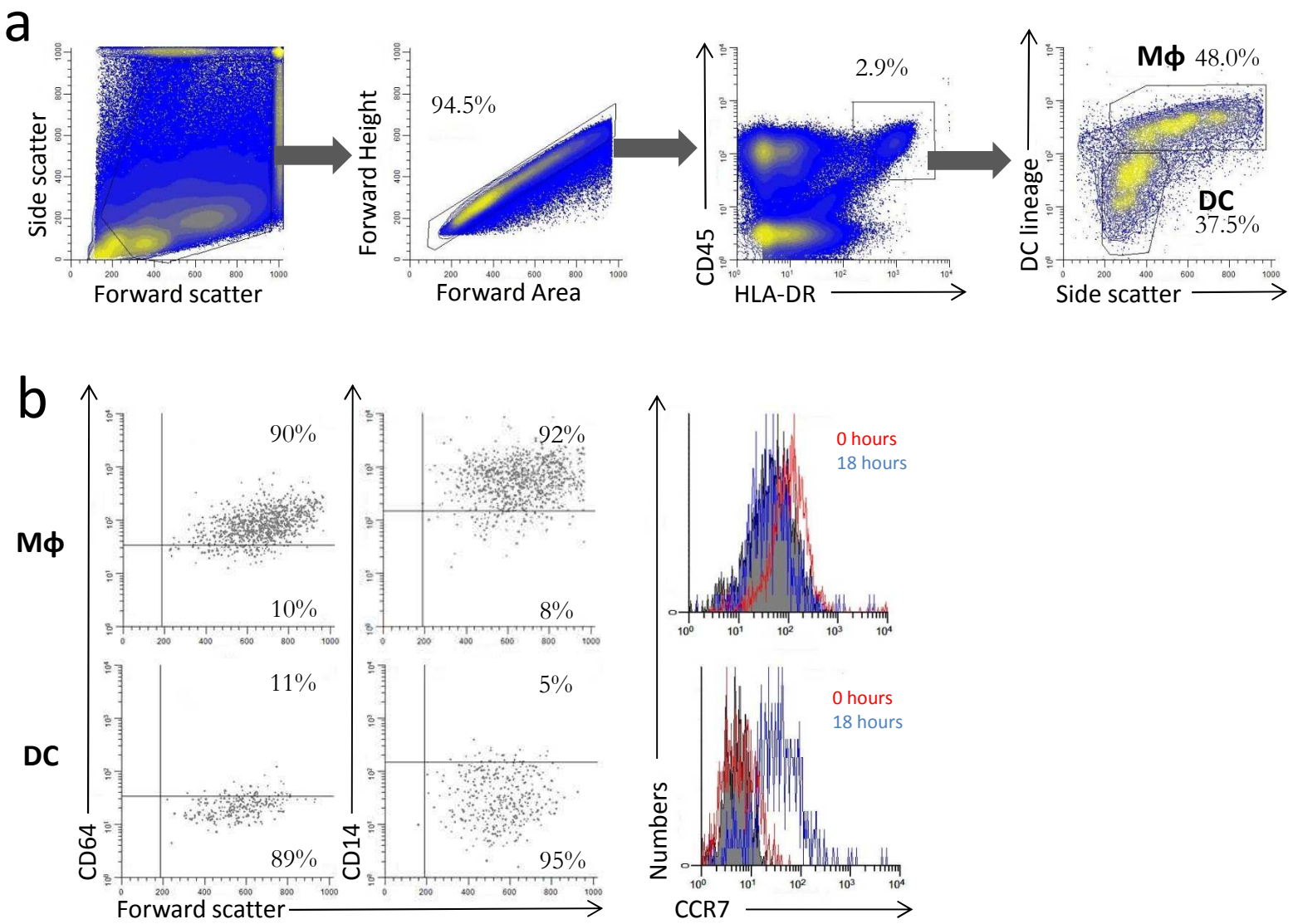
a
Side scatter
Forward scatter
Forward Height
94.5%
Forward Area
CD45
2.9%
HLA-DR
DC lineage
Mϕ 48.0%
DC
37.5%
Side scatter
b
Mϕ
DC
90%
10%
92%
8%
11%
89%
5%
95%
CD64
CD14
Forward scatter
0 hours
18 hours
0 hours
18 hours
Numbers
CCR7

FIGURE 1

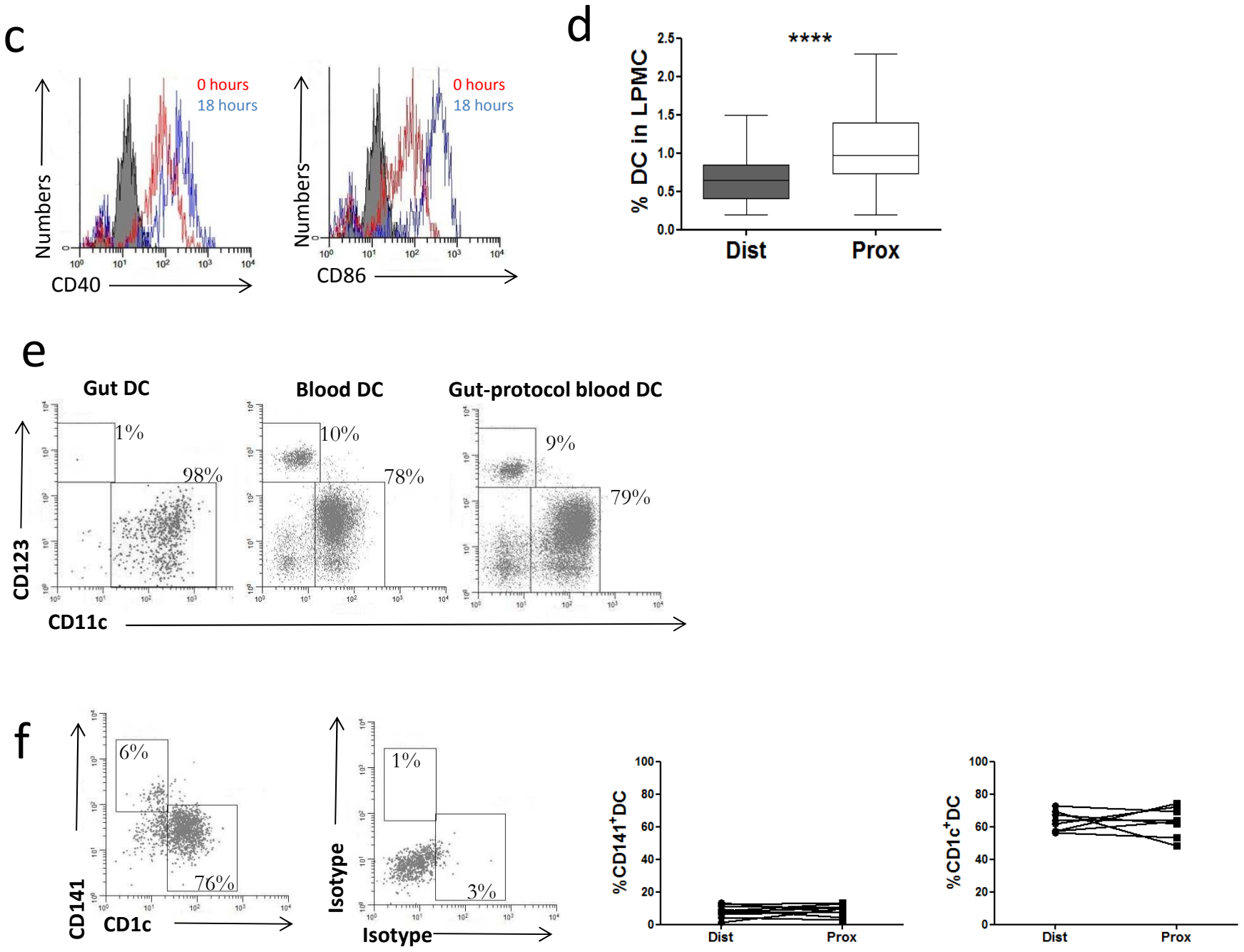
c
0 hours
18 hours
Numbers
CD40
0 hours
18 hours
Numbers
CD86
d
****
% DC in LPMC
2.5
2.0
1.5
1.0
0.5
0.0
Dist
Prox
e
Gut DC
Blood DC
Gut-protocol blood DC
1%
98%
10%
78%
9%
79%
CD123
CD11c
f
6%
76%
CD141
CD1c
1%
3%
Isotype
Isotype
%CD141+DC
100
80
60
40
20
0
Dist
Prox
%CD1c+DC
100
80
60
40
20
0
Dist
Prox

FIGURE 2

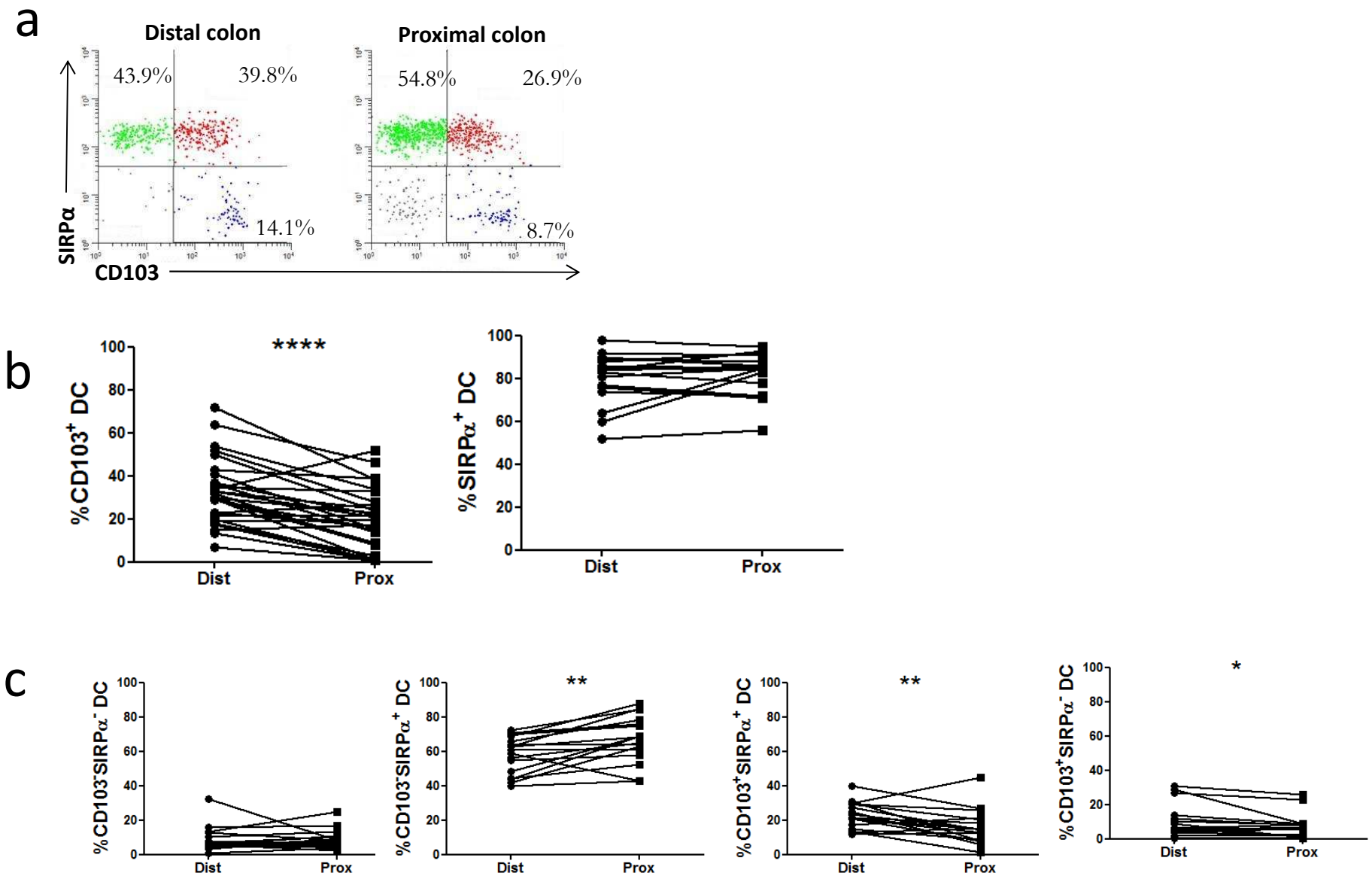
a
Distal colon
Proximal colon
43.9%
39.8%
14.1%
54.8%
26.9%
8.7%
SIRPα
CD103
b
****
%CD103+ DC
%SIRPα+ DC
Dist
Prox
c
%CD103-SIRPα- DC
%CD103-SIRPα+ DC
%CD103+SIRPα+ DC
%CD103+SIRPα- DC
**
**
*

FIGURE 2

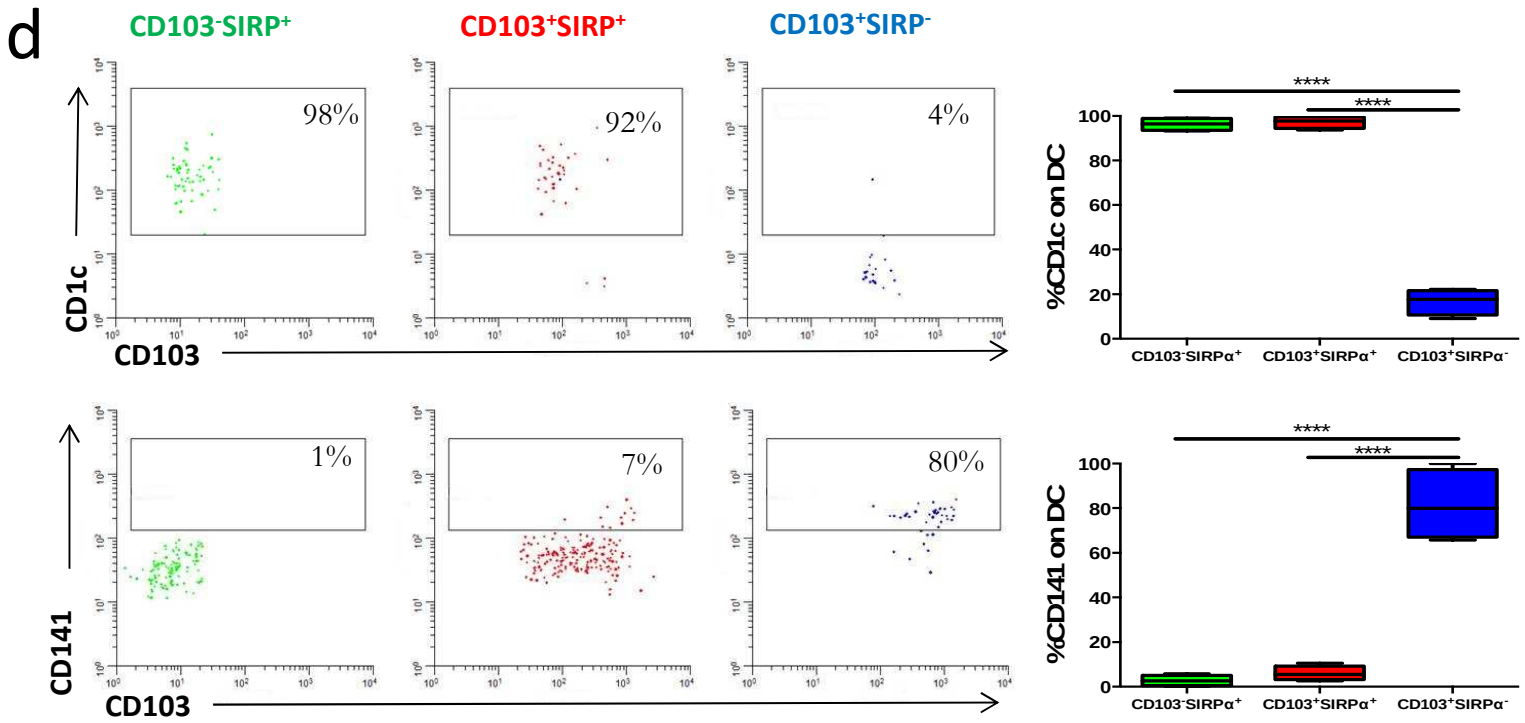
d
CD103-SIRP+
CD103+SIRP+
CD103+SIRP-
98%
92%
4%
CD1c
CD103
1%
7%
80%
CD141
CD103
%CD1c on DC
%CD141 on DC
****
****
100
80
60
40
20
0
CD103-SIRPα+
CD103+SIRPα+
CD103+SIRPα-

FIGURE 2

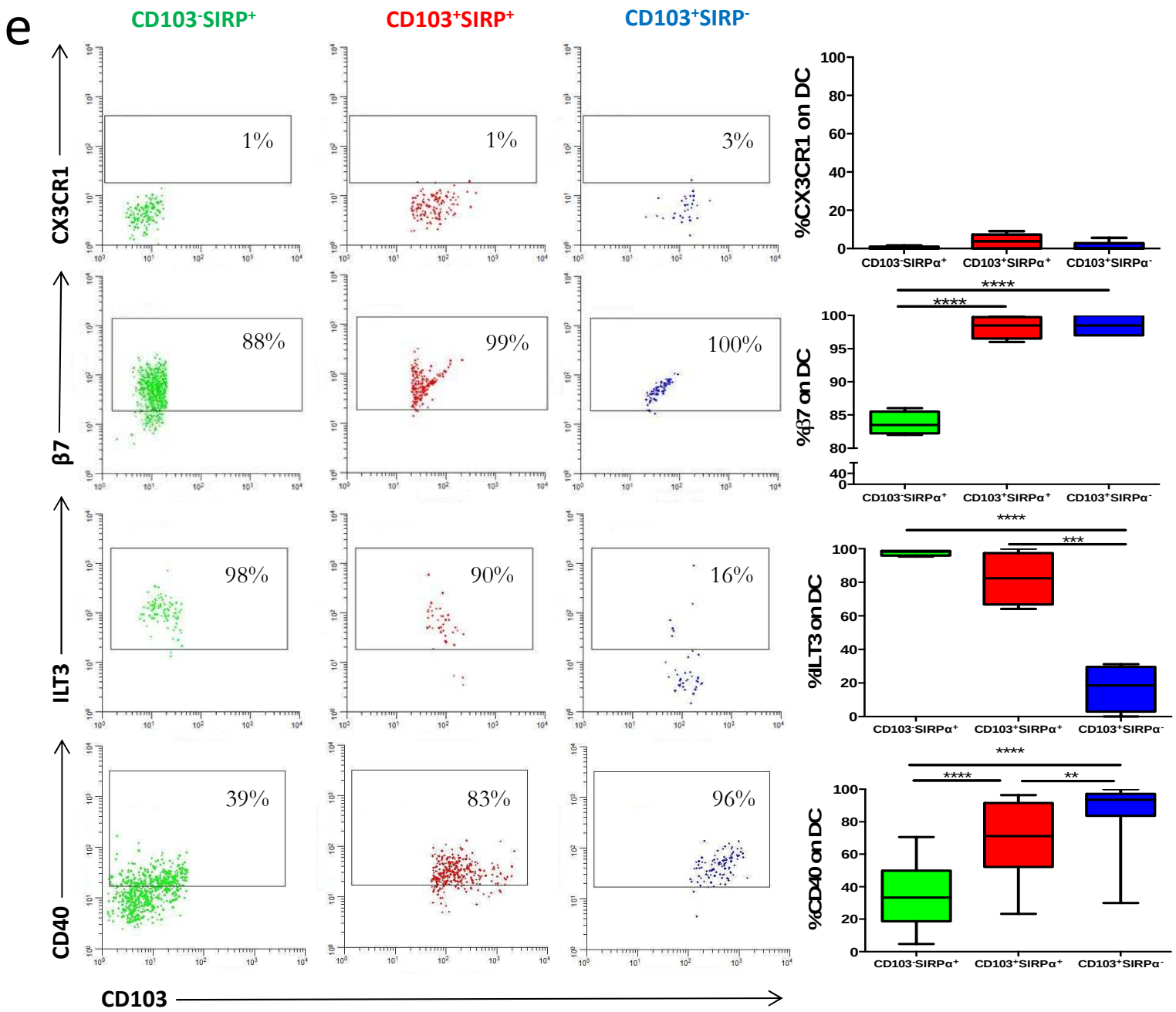
e
CD103-SIRP+
CD103+SIRP+
CD103+SIRP-
CX3CR1
β7
ILT3
CD40
CD103
1%
1%
3%
88%
99%
100%
98%
90%
16%
39%
83%
96%
%CX3CR1 on DC
%β7 on DC
%ILT3 on DC
%CD40 on DC
CD103-SIRPα+
CD103+SIRPα+
CD103+SIRPα-
****
***
**

FIGURE 2

f

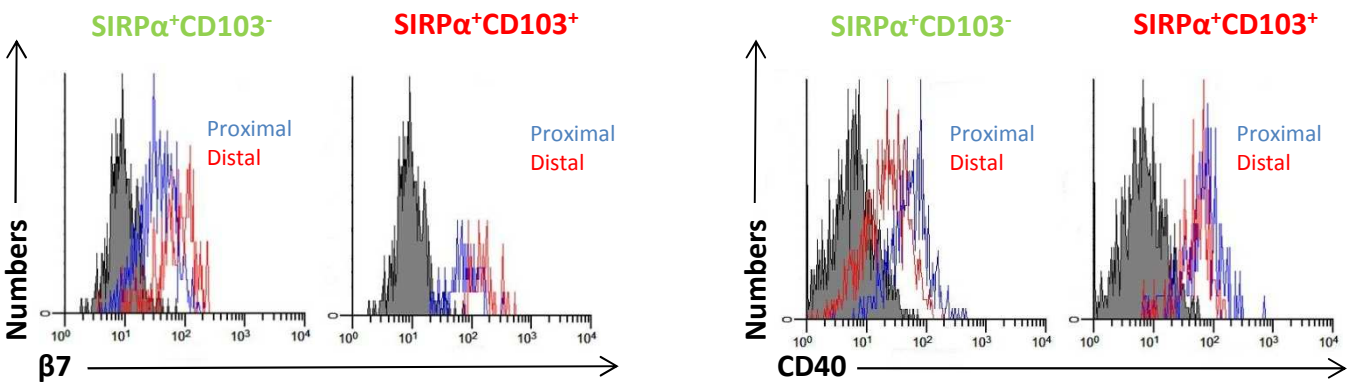
SIRPα+CD103-
SIRPα+CD103+
Proximal
Distal
Proximal
Distal
Numbers
β7
SIRPα+CD103-
SIRPα+CD103+
Proximal
Distal
Proximal
Distal
Numbers
CD40

FIGURE 3

a

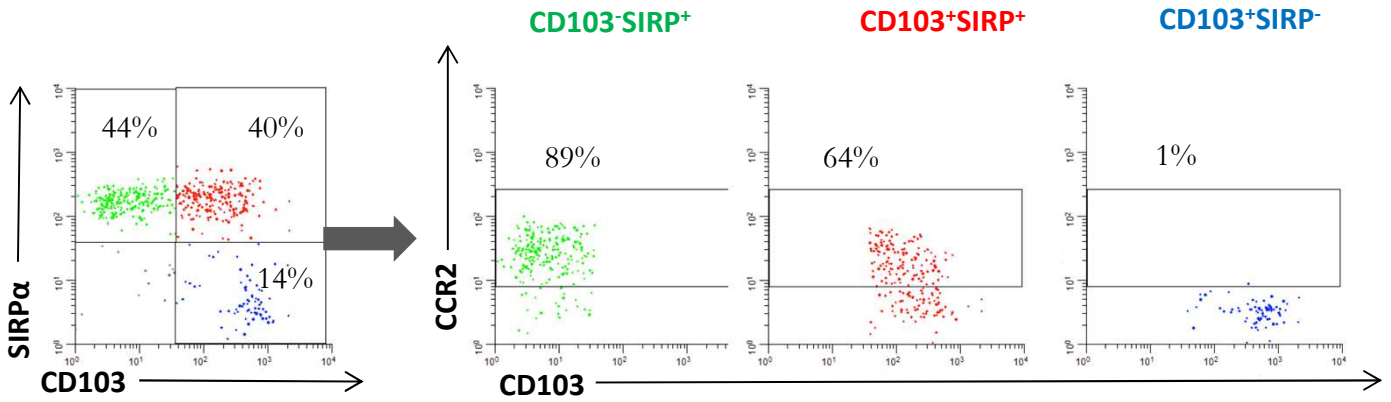
CD103⁻SIRP⁺
CD103⁺SIRP⁺
CD103⁺SIRP⁻
44%
40%
14%
SIRPα
CD103
89%
64%
1%
CCR2
CD103

b

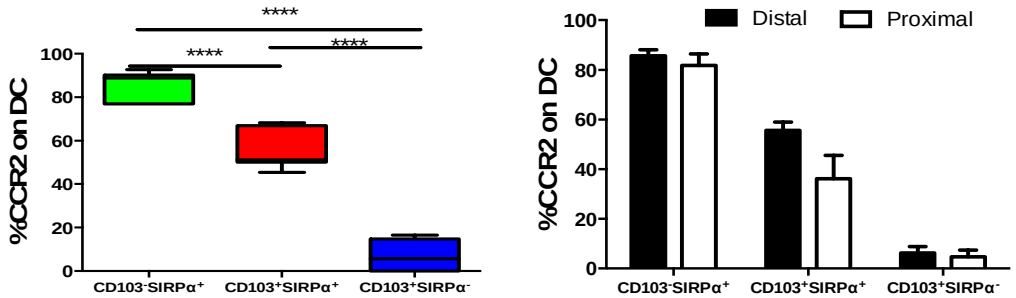
****
****
****
100
80
60
40
20
0
%CCR2 on DC
CD103⁻SIRPα⁺
CD103⁺SIRPα⁺
CD103⁺SIRPα⁻
Distal
Proximal
100
80
60
40
20
0
%CCR2 on DC
CD103⁻SIRPα⁺
CD103⁺SIRPα⁺
CD103⁺SIRPα⁻

FIGURE 3

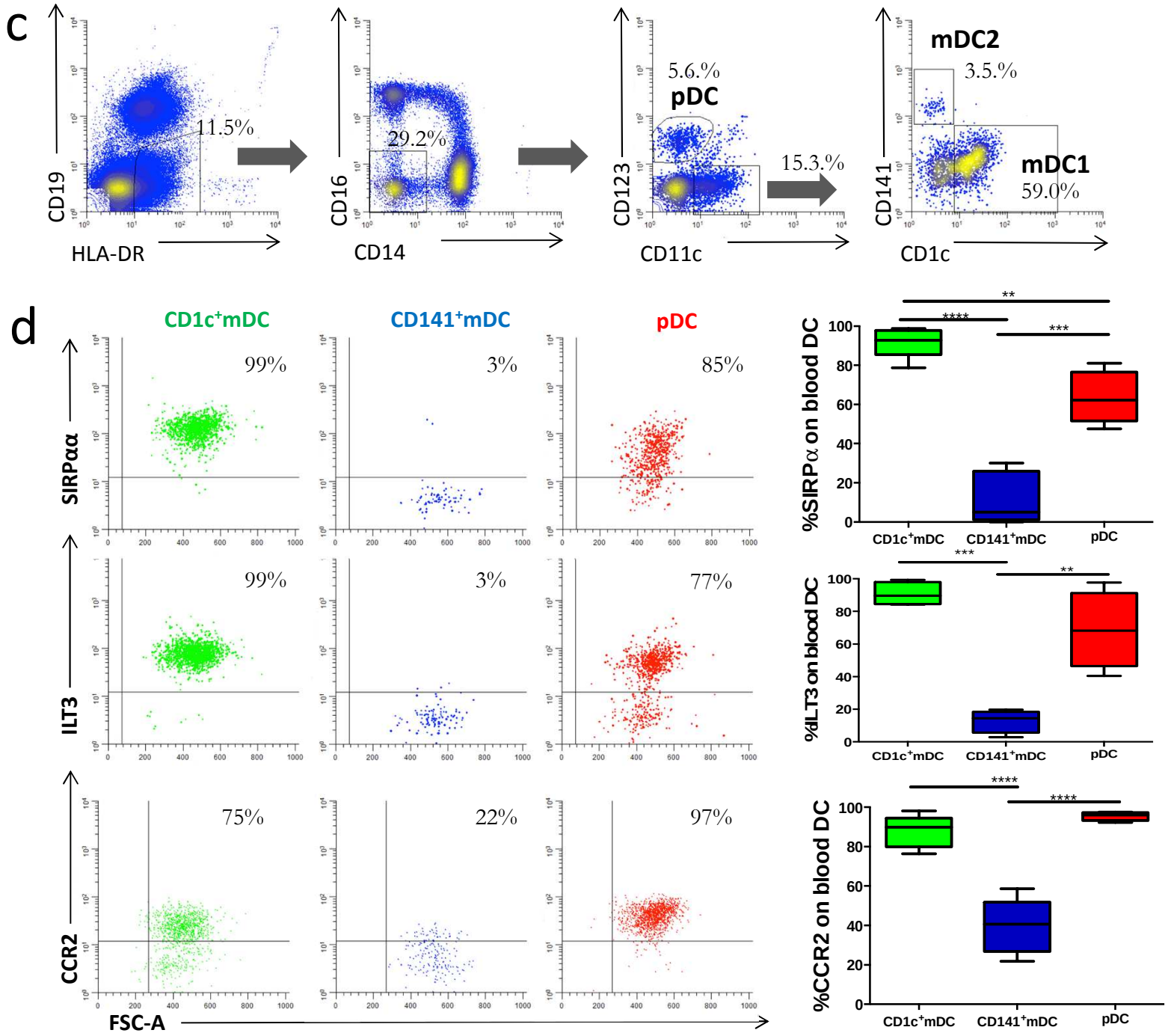
c
CD19
HLA-DR
11.5%
CD16
CD14
29.2%
CD123
CD11c
5.6%
pDC
15.3%
CD141
CD1c
mDC2
3.5%
mDC1
59.0%
d
CD1c+mDC
CD141+mDC
pDC
SIRPαα
99%
3%
85%
ILT3
99%
3%
77%
CCR2
75%
22%
97%
FSC-A
%SIRPα on blood DC
%ILT3 on blood DC
%CCR2 on blood DC
**
****
***
CD1c+mDC
CD141+mDC
pDC

FIGURE 3

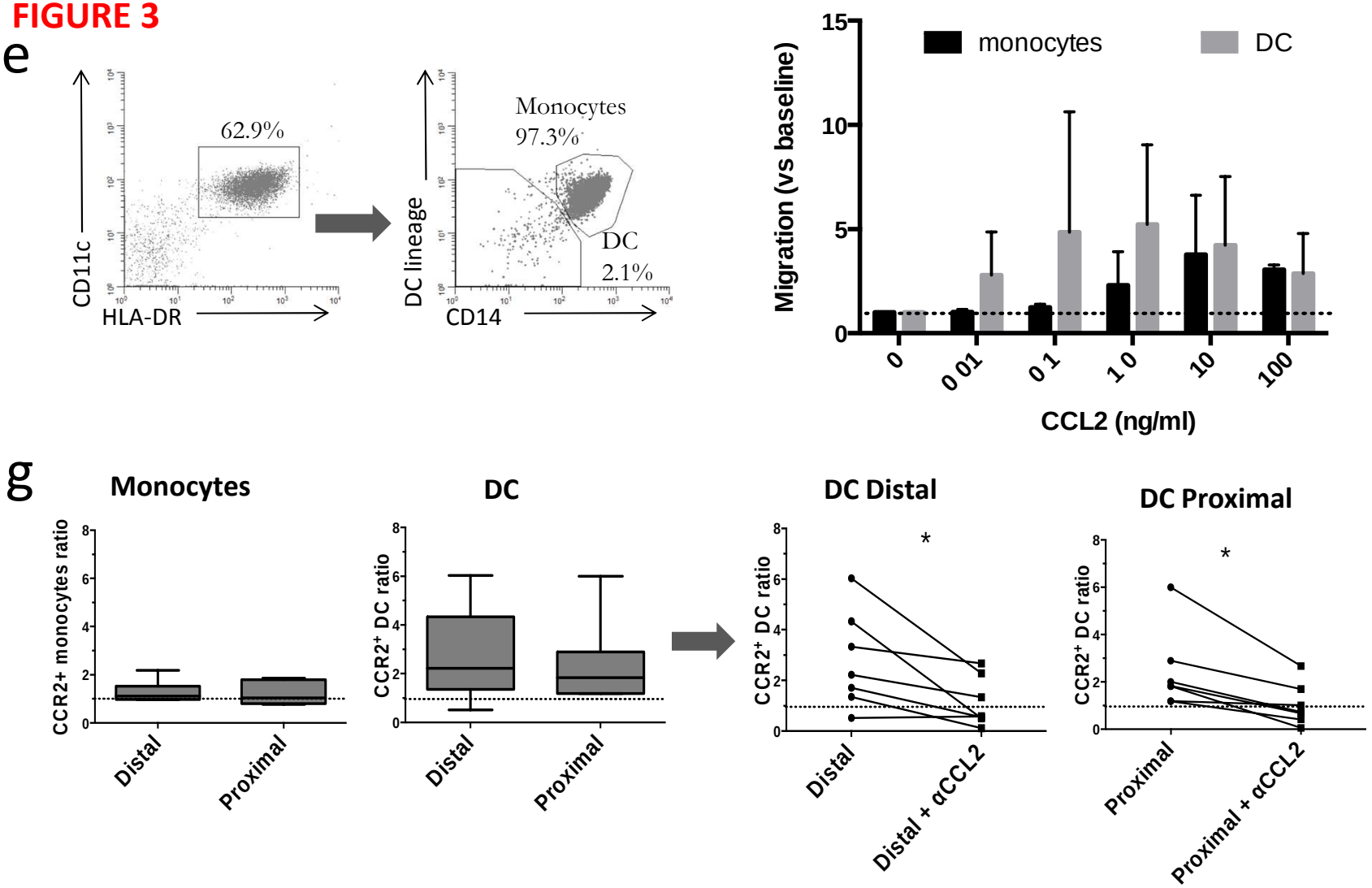
e
62.9%
CD11c
HLA-DR
Monocytes
97.3%
DC
2.1%
DC lineage
CD14
monocytes
DC
Migration (vs baseline)
CCL2 (ng/ml)
g
Monocytes
DC
DC Distal
DC Proximal
CCR2+ monocytes ratio
CCR2+ DC ratio
Distal
Proximal
Distal + αCCL2
Proximal + αCCL2
*

Figure 4

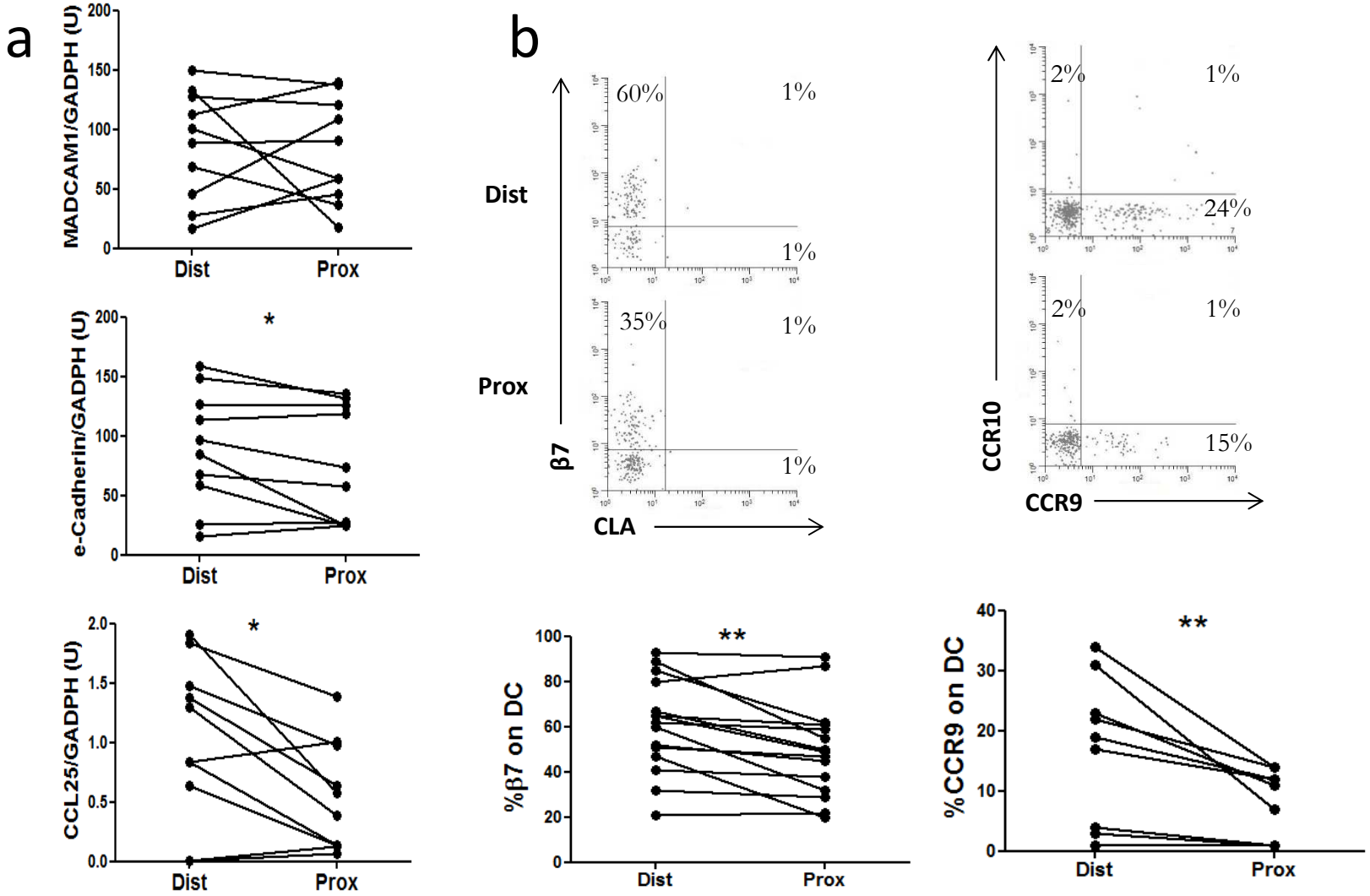
a
MADCAM1/GADPH (U)
200
150
100
50
0
Dist
Prox
e-Cadherin/GADPH (U)
*
CCL25/GADPH (U)
2.0
1.5
1.0
0.5
0.0
b
Dist
Prox
β7
CLA
60%
1%
35%
1%
1%
1%
CCR10
CCR9
2%
1%
24%
2%
1%
15%
%β7 on DC
**
%CCR9 on DC
40
30
20
10
0

Figure 4

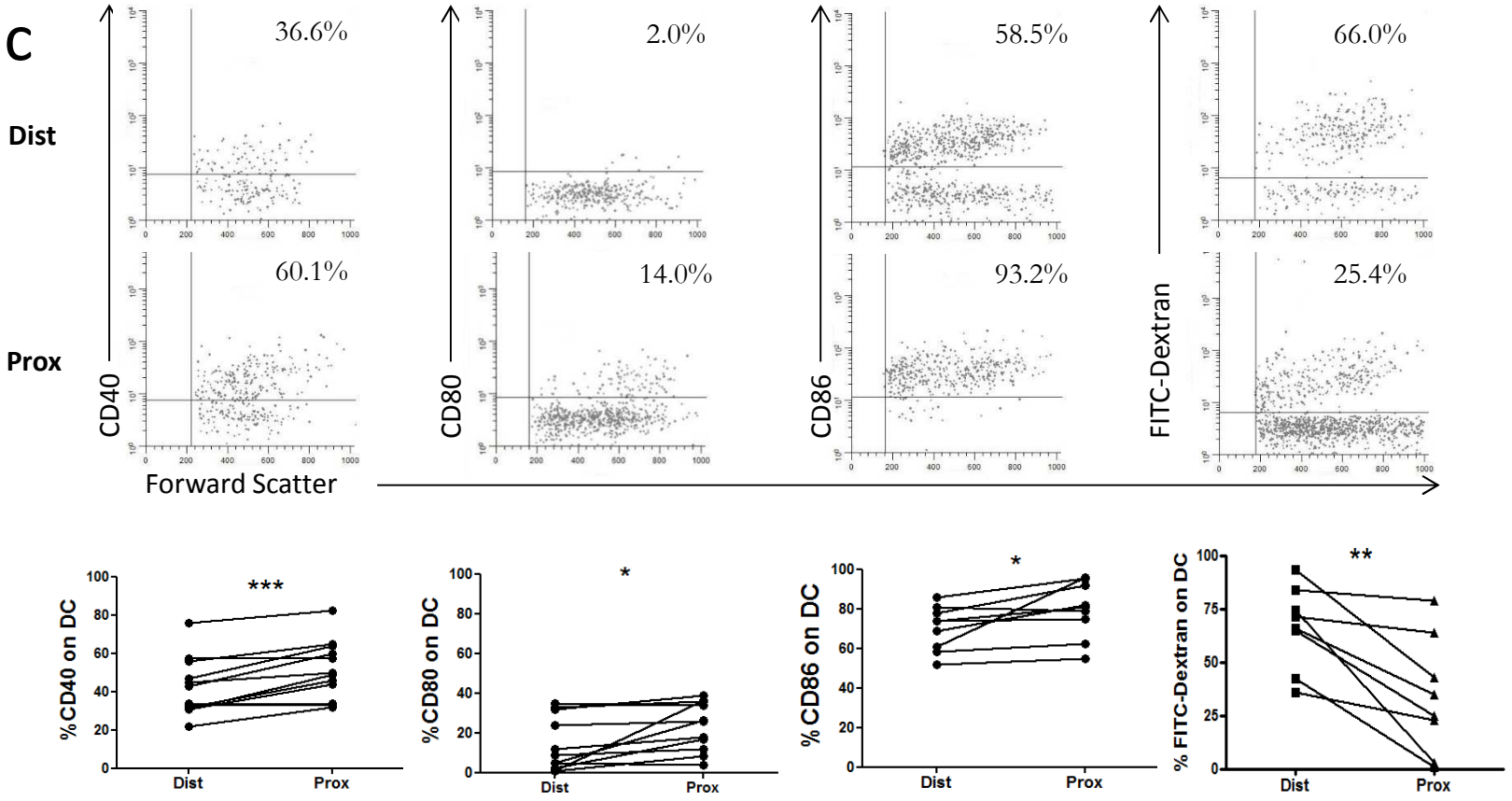
C
Dist
Prox
36.6%
2.0%
58.5%
66.0%
60.1%
14.0%
93.2%
25.4%
CD40
CD80
CD86
FITC-Dextran
Forward Scatter
% CD40 on DC
% CD80 on DC
% CD86 on DC
% FITC-Dextran on DC
***
*
*
**
Dist
Prox

Figure 4

d

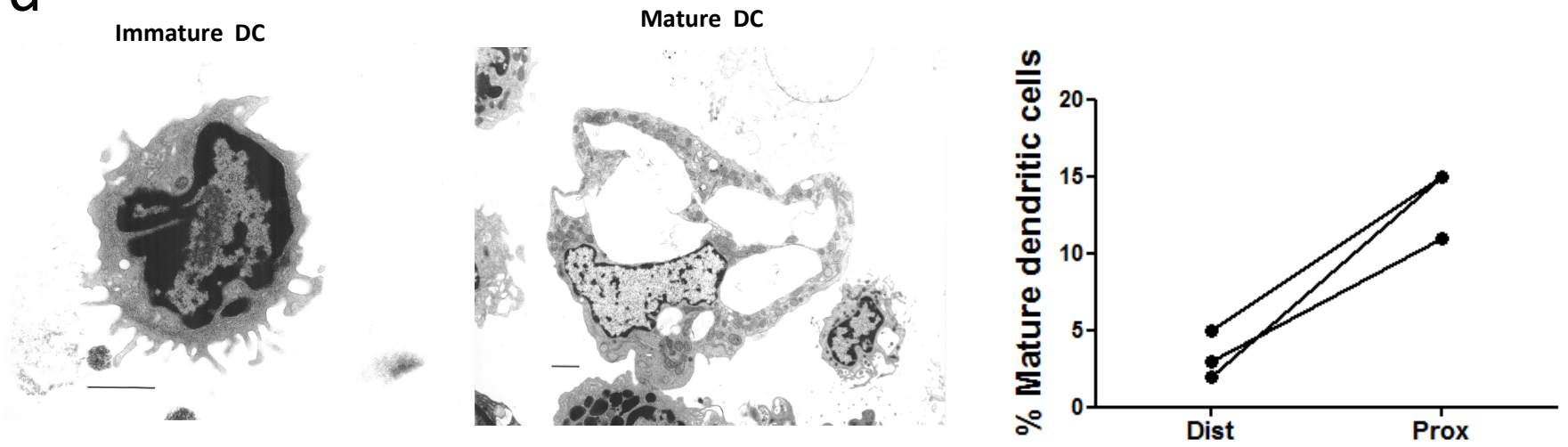
Immature DC
Mature DC
% Mature dendritic cells
20
15
10
5
0
Dist
Prox

Figure 5

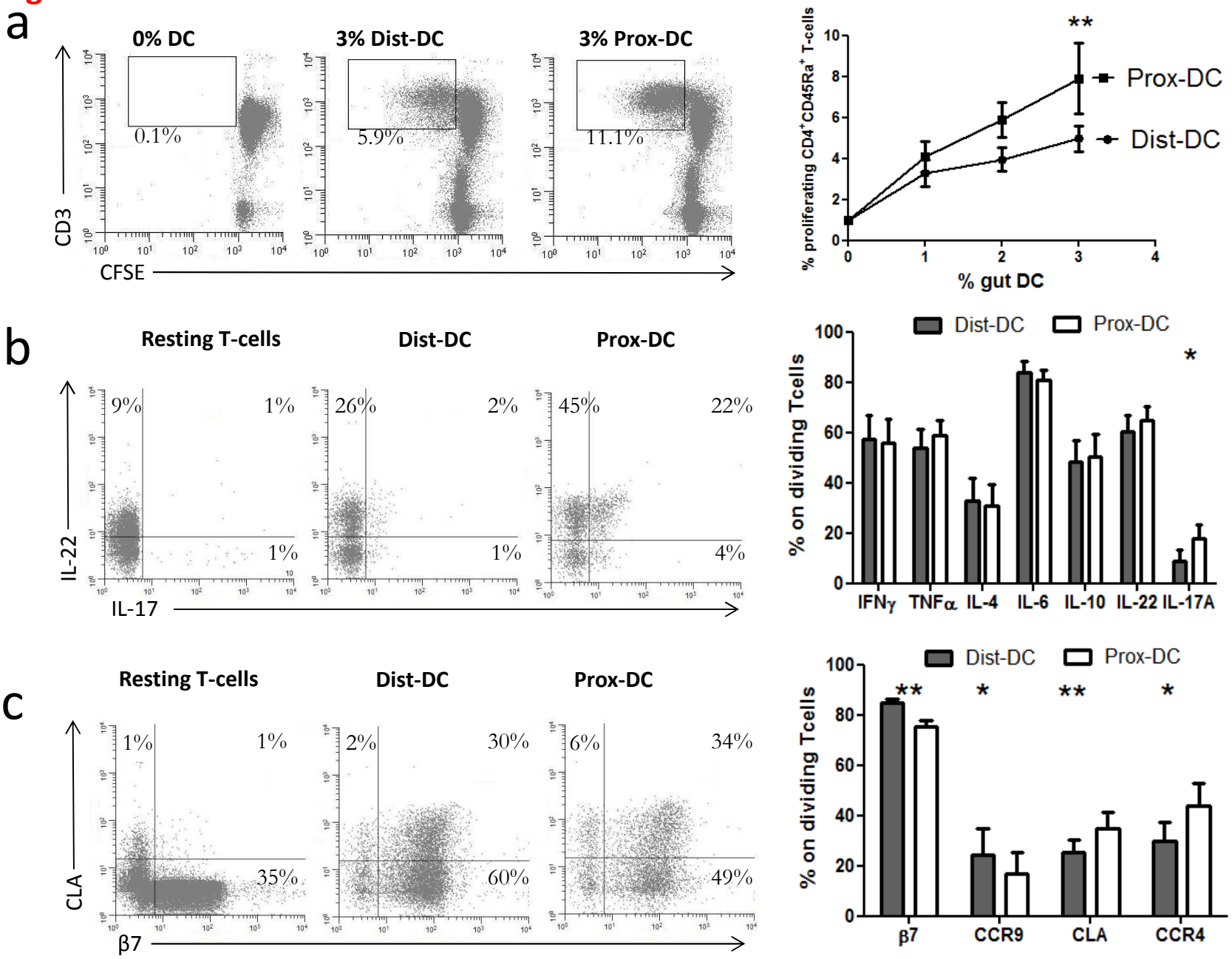
a
0% DC
3% Dist-DC
3% Prox-DC
0.1%
5.9%
11.1%
CD3
CFSE
% proliferating CD4+CD45Ra+ T-cells
% gut DC
Prox-DC
Dist-DC
**
b
Resting T-cells
Dist-DC
Prox-DC
9%
1%
1%
26%
2%
1%
45%
22%
4%
IL-22
IL-17
% on dividing Tcells
IFNγ
TNFα
IL-4
IL-6
IL-10
IL-22
IL-17A
*
c
Resting T-cells
Dist-DC
Prox-DC
1%
1%
35%
2%
30%
60%
6%
34%
49%
CLA
β7
% on dividing Tcells
**
*
**
*
β7
CCR9
CLA
CCR4

FIGURE 6

a

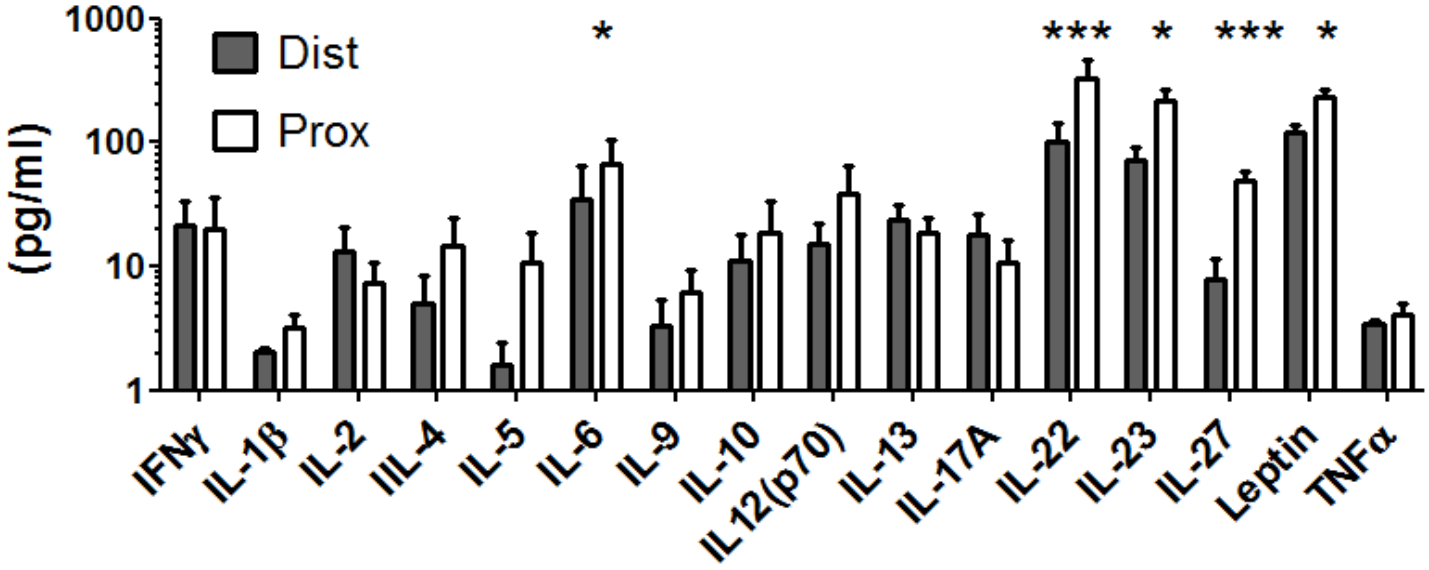

b

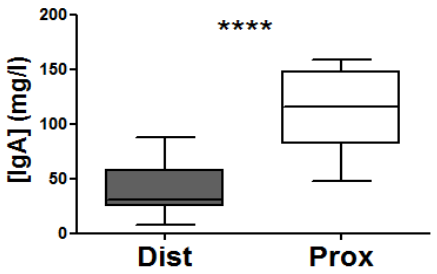

c

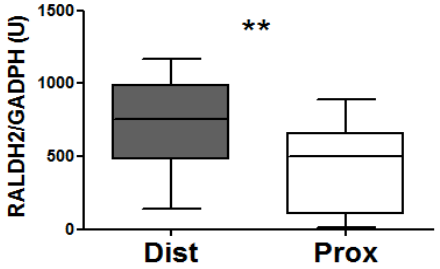

d

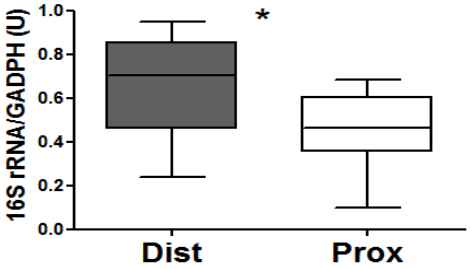

FIGURE 6

e

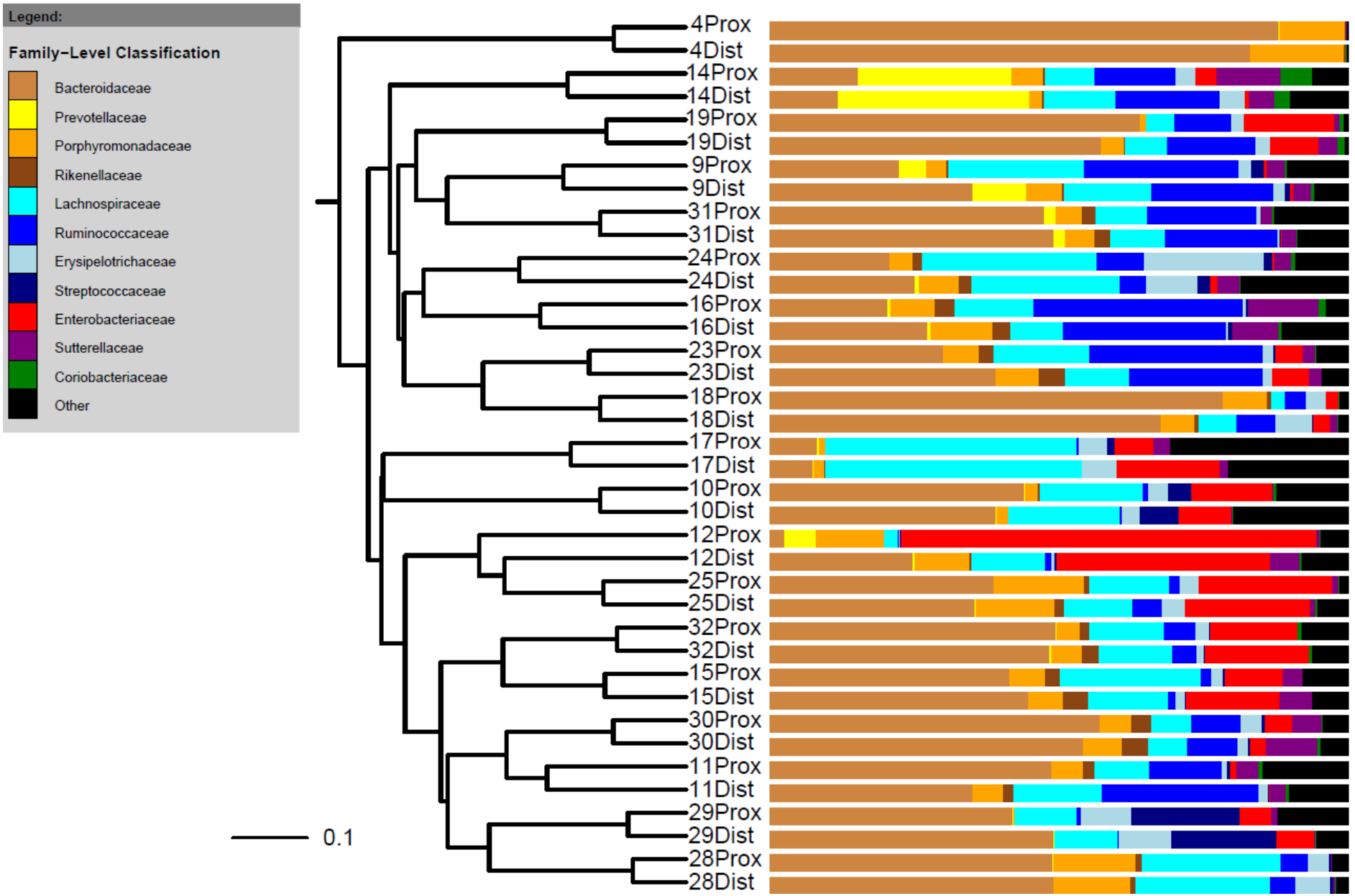
Legend:
Family−Level Classification
Bacteroidaceae
Prevotellaceae
Porphyromonadaceae
Rikenellaceae
Lachnospiraceae
Ruminococcaceae
Erysipelotrichaceae
Streptococcaceae
Enterobacteriaceae
Sutterellaceae
Coriobacteriaceae
Other
4Prox
4Dist
14Prox
14Dist
19Prox
19Dist
9Prox
9Dist
31Prox
31Dist
24Prox
24Dist
16Prox
16Dist
23Prox
23Dist
18Prox
18Dist
17Prox
17Dist
10Prox
10Dist
12Prox
12Dist
25Prox
25Dist
32Prox
32Dist
15Prox
15Dist
30Prox
30Dist
11Prox
11Dist
29Prox
29Dist
28Prox
28Dist
0.1

SUPPLEMENTARY MATERIALS

Murine Experiments

Conventionally raised and germ free (reared from germ free breeding pairs) male C57BL/6 mice were sacrificed at 8 weeks of age and lamina propria cells isolated for flow cytometry analysis. Briefly; proximal and distal large intestine was chopped into small pieces and incubated with vigorous stirring (200 rpm) in complete media with 2 mM EDTA for 15 minutes at 37 ºC. This was repeated, then colon pieces were recovered and incubated for 40 minutes at 37 ºC with collagenase (type VIII, Sigma, 100 U/mL). The lamina propria cells were then filtered, washed and stained for flow cytometry analysis on a BD Fortessa instrument and Flowjo software (Treestar). Antibodies used were: CD45 (clone 20-F11, Biolegend), MHCII (clone 2G9, BD), and CD11c (clone N418, Ebioscience). Staining was done at 4 ºC in the presence of Fc receptor block (anti-CD16/32, clone 93, Biolegend). Zombie AQUA (Biolegend) was used for live-dead discrimination according to manufacturer's directions. All experiments were carried out with UK Home Office approval.

Supplementary Table 1: Antibodies and flow cytometry

Antibody Specificity	Clone	Conjugate	Manufacturer
β7	FIB504	PE	BD
CCR2	K036C2	PE-Cy7	Biolegend
	K036C2	APC	Biolegend
	48607	Alexa 647	BD
CCR4	205410	APC	R&D
CCR7	150503	PE	R&D
CCR8	191704	APC	R&D
CCR9	248621	PE	R&D
CCR10	314305	APC	R&D
CD1c (BDCA1)	AD5-8E7	FITC	Miltenyi
	AD5-8E7	PE	Miltenyi
	L161	Alexa700	Biolegend
CD3	UCHT1	PE-Cy5	BD
CD11c	KB90	FITC	Dako
	B-Ly6	PE	BD
	3.9	PE-Cy7	eBioscience
	B-Ly6	BV605	BD
	Bu15	APC-Cy7	Biolegend
CD14	M5E2	PE	BD
	TÜK4	PE-Cy5	Serotec
	MΦP9	PE-CF594	BD
CD16	3G8	PE-Cy5	BD
CD19	HIB19	PE-Cy5	BD
CD34	581	PE-Cy5	BD
CD40	LOB7/6	FITC	BD
	LOB7/6	PE	BD
CD45	HI30	PE-Cy7	BD
	VS143	APC-Cy7	Biolegend
	HI30	PE-Cy7	Biolegend
	HI30	BUV395	BD
CD64	10.1	PE-Cy5	Abcam
	10.1	PE-Cy7	Biolegend
CD80	L307.4	FITC	BD
	L307.4	PE	BD
CD86	BU63	FITC	Serotec
CD103	Ber-ACT8	FITC	BD
	Ber-ACT8	PE	Biolegend
	Ber-ACT8	BV421	BD
	Ber-ACT8	PE-Cy7	Biolegend
CD123	6H6	PE-Cy7	eBioscience
	7G3	BV786	BD
CD141 (BDCA3)	501733	FITC	R&D
	1A4	BV711	BD

	AD5-14H12	PE	Miltenyi
CD172a (SIRPα)	602411	FITC	R&D
	602411	PE	R&D
	SE5A5	PE-Cy7	Biolegend
CD209 (DC-SIGN)	120507	FITC	R&D
	120507	PE	R&D
CD303 (BDCA2)	AC144	FITC	Miltenyi
CLA	HECA-452	APC	BD
	HECA-452	Biotin	BD
CX3CR1	528728	PE	R&D
HLA-DR	G46-6	APC	R&D
	L243	BV570	Biolenged
IFNγ	25723.11	APC	BD
IL-4	8DA-8	PE-Cy7	eBioscience
IL-6	AS12	FITC	eBioscience
	1936	PE	R&D
IL-10	BT-10	FITC	eBioscience
	JES3-9D7	PE-Cy7	eBioscience
	JES3-19F1	APC	BD
IL-17A	eBIO64DEC17	APC	eBioscience
IL-22	22URTI	APC	eBioscience
	IL22JOP	PE-Cy7	eBioscience
ILT3	293623	PE	R&D
Streptavidin	not applied	APC	BD
TGFβ	35409	PE	R&D
TLR2	TLR2.3	FITC	Serotec
TLR4	HTA125	FITC	Serotec
TNFα	B-D9	FITC	Serotec
	Mab11	PE-Cy7	eBioscience

Supplementary Table 2: quantitative PCR primers

Molecule	Primers sequence	Ta	Primer source
GADPH	Fw 5'-GAAGGTGAAGGTCGGAGTC-3' Rv 5'-GAAGATGGTGATGGGATTTC-3'	60	Ren et al, 2005[1]
16S rRNA	Fw 5'-TTAAACTCAAAGGAATTGACGG-3' Rv 5'-CTCACGRCACGAGCTGACGAC-3'	68	Ozbek et al, 2009[2]
RALDH2	5532957001_Roche	60	Roche
CCL25	Fw 5'-GATAAAACCGTCGCCCTACA-3' Rv 5'-TCCTTTGGGTCTGCACATAGC-3'	58	NCBI Reference Sequence: NM_005624.3
MADCAM1	Fw 5´-CTGTACGGCCCACAAAGTCA-3´ Rv 5´-TCTGTCACCCTGAACAGCAC-3´	60	NCBI Reference Sequence: NM_130760.2
e-cadherin	Fw 5´-CAGTCTCTTCTCTCACGCGT-3´ Rv 5´-TGAGGATGGTGTAAGCGATGG-3´	60	NCBI Reference Sequence: NM_004360.3

Primers used for quantitative PCR including primer sequence or source and annealing temperature (Ta). Primers for CCL25, MADCAM1 and e-cadherin were designed with Primer-BLAST[3] (http://www.ncbi.nlm.nih.gov/tools/primer-blast/) using the reference sequences provided in the table.

Supplementary Table 3: ENA accession number information for each of the biopsy tissue sample sequencing results from the microbiota analyses. Samples marked L are from the left or distal colon, those marked R are from the right or proximal colon.

Sample name	Biopsy sample info	ENA sample accession number
4L	Patient 4 - distal colon	ERS557964
4R	Patient 4 - proximal colon	ERS557965
9L	Patient 9 - distal colon	ERS557966
9R	Patient 9 - proximal colon	ERS557967
10L	Patient 10 - distal colon	ERS557968
10R	Patient 10 - proximal colon	ERS557969
11L	Patient 11 - distal colon	ERS557970
11R	Patient 11 - proximal colon	ERS557971
12L	Patient 12 - distal colon	ERS557972
12R	Patient 12 - proximal colon	ERS557973
14L	Patient 14 - distal colon	ERS557974
14R	Patient 14 - proximal colon	ERS557975
15L	Patient 15 - distal colon	ERS557976
15R	Patient 15 - proximal colon	ERS557977
16L	Patient 16 - distal colon	ERS557978
16R	Patient 16 - proximal colon	ERS557979
17L	Patient 17 - distal colon	ERS557980
17R	Patient 17 - proximal colon	ERS557981
18L	Patient 18 - distal colon	ERS557982
18R	Patient 18 - proximal colon	ERS557983
19L	Patient 19 - distal colon	ERS557984
19R	Patient 19 - proximal colon	ERS557985
23L	Patient 23 - distal colon	ERS557986
23R	Patient 23 - proximal colon	ERS557987
24L	Patient 24 - distal colon	ERS557988
24R	Patient 24 - proximal colon	ERS557989
25L	Patient 25 - distal colon	ERS557990
25R	Patient 25 - proximal colon	ERS557991
28L	Patient 28 - distal colon	ERS557992
28R	Patient 28 - proximal colon	ERS557993
29L	Patient 29 - distal colon	ERS557994
29R	Patient 29 - proximal colon	ERS557995
30L	Patient 30 - distal colon	ERS557996
30R	Patient 30 - proximal colon	ERS557997
31L	Patient 31 - distal colon	ERS557998
31R	Patient 31 - proximal colon	ERS557999
32L	Patient 32 - distal colon	ERS558000
32R	Patient 32 - proximal colon	ERS558001

Supplementary Figure 1:

Dendritic cells (DC) were identified as in Figure 1a and divided into subsets based on expression of CD103 and SIRPα. CCR2 expression was determined in each DC subset using two different clones labelled with different fluorochormes: **(a)** clone 48607 labelled in Alexa 647 and **b)** clone K036C2 labelled in PE-Cy7. Results are representative of two independent experiments performed with similar results.

Supplementary Figure 2: Dendritic cell compartmentalization in the murine colon is modulated by the microbiota

Dendritic cells (DC) from proximal (Prox) and distal (Dist) regions of the colon in conventional (Conv) and germ free (GF) mice were identified by flow cytometry within single colonic viable cells (ZombieAqua$^-$CD45$^+$) and mean frequencies (with SD) displayed. Results are representative of 2 independent experiments (n=5 mice per group in each experiment). One-way ANOVA with Tukey's multiple comparisons was applied and p-values <0.05 were considered significant (*p<0.05, pair-wise comparisons without * were not significant).

REFERENCES

1. Ren M, Pozzi S, Bistulfi G, et al. Impaired retinoic acid (RA) signal leads to RARbeta2 epigenetic silencing and RA resistance. Mol Cell Biol 2005;25:10591-603.
2. Ozbek SM, Ozbek A, Erdorgan AS. Analysis of Enterococcus faecalis in samples from Turkish patients with primary endodontic infections and failed endodontic treatment by real-time PCR SYBR green method. J Appl Oral Sci 2009;17:370-4.
3. Ye J, Coulouris G, Zaretskaya I, et al. Primer-BLAST: a tool to design target-specific primers for polymerase chain reaction. BMC Bioinformatics 2012;13:134.

Supplementary figure 1

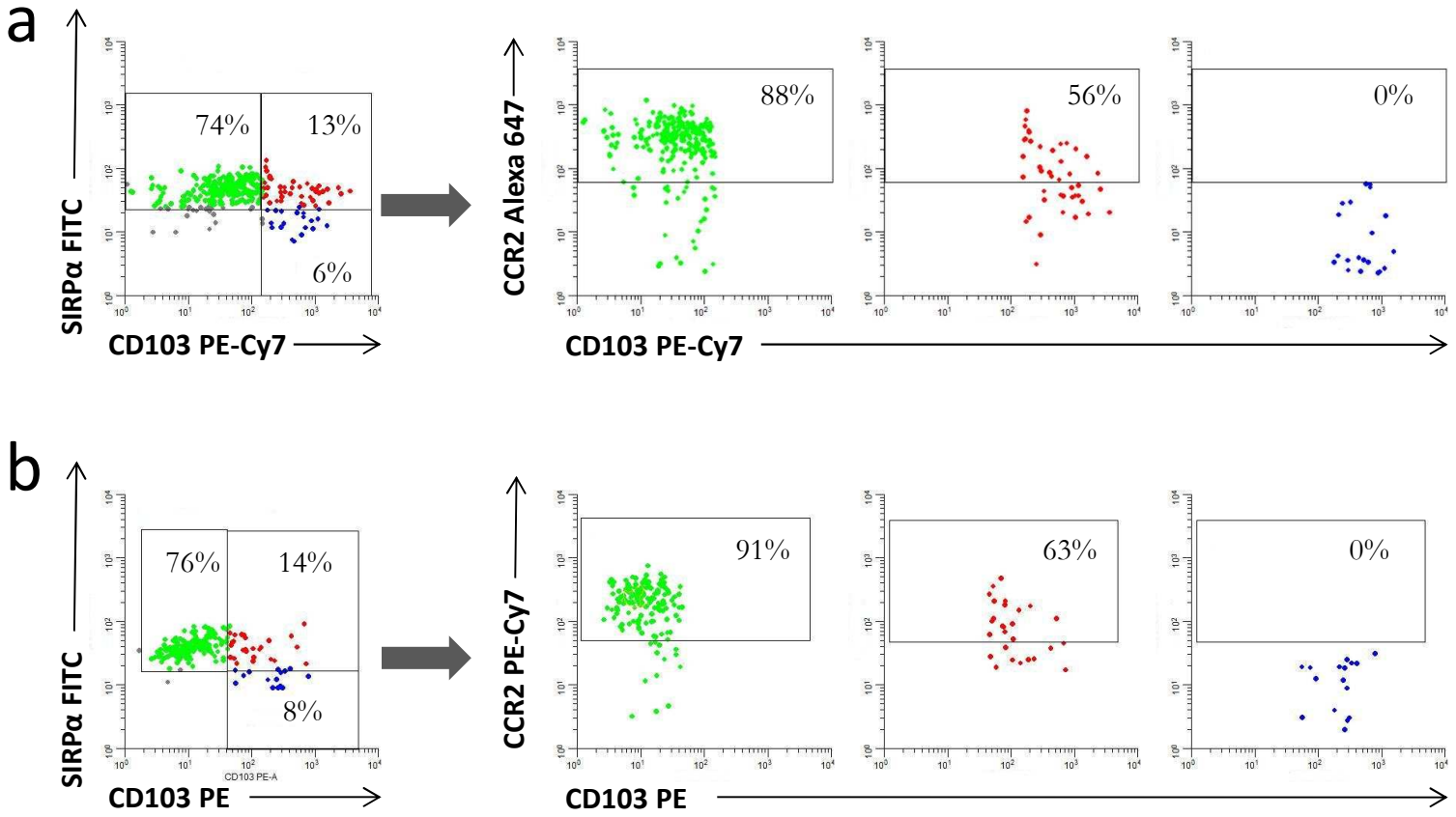

Supplementary figure 2